

Review

Textiles for Very Cold Environments

Tomasz Blachowicz ^{1,*}, Maciej Malczyk ¹, Ilda Kola ², Guido Ehrmann ³, Eva Schwenzfeier-Hellkamp ⁴
and Andrea Ehrmann ⁴

¹ Institute of Physics—Center for Science and Education, Silesian University of Technology, 44-100 Gliwice, Poland

² Department of Textile and Fashion, Polytechnic University of Tirana, 1019 Tirana, Albania; ikola@fim.edu.al

³ Virtual Institute of Applied Research on Advanced Materials (VIARAM)

⁴ Institute for Technical Energy Systems (ITES), Bielefeld University of Applied Sciences and Arts, 33619 Bielefeld, Germany; eva.schwenzfeier-hellkamp@hsbi.de (E.S.-H.); andrea.ehrmann@hsbi.de (A.E.)

* Correspondence: tomasz.blachowicz@polsl.pl

Abstract: Textiles are often used to protect people from cold environments. While most garments are designed for temperatures not far below 0 °C, very cold regions on the earth near the poles or on mountains necessitate special clothing. The same is true for homeless people who have few possibilities to warm up or workers in cooling chambers and other cold environments. Passive insulating clothing, however, can only retain body heat. Active heating, on the other hand, necessitates energy, e.g., by batteries, which are usually relatively heavy and have to be recharged regularly. This review gives an overview of energy-self-sufficient textile solutions for cold environments, including energy harvesting by textile-based or textile-integrated solar cells; piezoelectric sensors in shoes and other possibilities; energy storage in supercapacitors or batteries; and heating by electric energy or phase-change materials.

Keywords: personal protective equipment; energy harvesting; energy storage; heating; flexible solar cells; temperature sensors



Citation: Blachowicz, T.; Malczyk, M.; Kola, I.; Ehrmann, G.; Schwenzfeier-Hellkamp, E.; Ehrmann, A. Textiles for Very Cold Environments. *Processes* **2024**, *12*, 927. <https://doi.org/10.3390/pr12050927>

Academic Editors: Zhanxiao Kang and Qing Chen

Received: 11 April 2024

Revised: 28 April 2024

Accepted: 29 April 2024

Published: 1 May 2024



Copyright: © 2024 by the authors. Licensee MDPI, Basel, Switzerland. This article is an open access article distributed under the terms and conditions of the Creative Commons Attribution (CC BY) license (<https://creativecommons.org/licenses/by/4.0/>).

1. Introduction

Keeping people warm in a cold environment is one of the main purposes of clothes. While thousands of years ago, natural fibers from animals and plants, as well as fur parts, were woven into warming garments [1], nowadays, chemical fibers are being investigated more and more regarding their applicability in warming clothes [2–4]. Besides passive warming by reflecting thermal radiation back towards the human body [5,6], creating air layers as insulation to reduce heat convection [7,8] or increasing the ratio of absorbed thermal radiation from the sun [9,10], there are nowadays many attempts to provide active heating.

Amongst the physical effects that can be used for heating up garments, there are phase-change materials (PCMs) [11–13], as well as different possibilities for converting electric energy into heat [14–16]. While the first are energy-self-sufficient, they have the disadvantage that they can only work in a material-dependent temperature range and cannot be controlled by the user. Electric heating of garments, also called Joule heating [17], on the other hand, needs the possibility of storing electric energy in batteries or supercapacitors to make it available when it is needed and ideally to harvest energy by the garment to make it independent from external power supplies.

This review gives an overview of recent research regarding energy-self-sufficient textiles for active heating to protect people from very cold environments, such as workers in cold storage houses, astronauts, people living near the poles or homeless people. The next sections review different possibilities for actively heating textiles by PCMs or electrically to harvest and store energy in textiles, and then the main part discusses recent research on energy-self-sufficient heating textiles and their potential applications.

2. Active Heating with Textiles

Active heating always requires energy, usually either in the form of electric energy or as latent heat stored in PCMs or subcooled liquids, whereupon the latter are usually not applied in textile fabrics but in simple heat pads activated by buckling a metal sheet. Here we give an overview of different ways of active heating with textile fabrics.

2.1. Phase-Change Materials

Phase-change materials can be integrated into textiles in the form of fibers, microcapsules or nanocapsules [18–20]. PCMs store a large amount of latent heat when molten and release it during solidifying [21]. This process, as shown in Figure 1, makes them especially interesting for textiles used in environments with fluctuating temperatures, e.g., for astronauts' space suits [22]. During melting or crystallization, the temperature of the PCM remains approx. constant. During an increase in temperature, the PCM can absorb heat that is stored in the liquefied phase, while decreasing external temperatures will lead to the release of this stored heat energy by the solidification of the PCM [23].

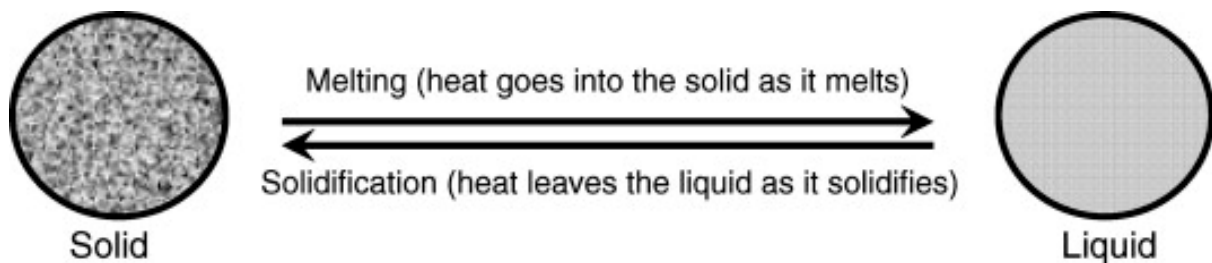


Figure 1. Schematic representation of phase-change process. Reprinted from [22], Copyright 2008, with permission from Elsevier.

Different materials have not only different temperature ranges for storing and releasing heat but also different energy storage properties. While water at 0 °C or even 100 °C can also be regarded as a PCM, several materials provide much higher energy storage capacity combined with high thermal conductivity in a suitable temperature range [24]. For paraffin waxes, Farid et al. reported melting temperatures of 44–64 °C and latent heats of 167–210 kJ/kg [25]. A better suitable temperature range of 30–65 °C was found for fatty acids, which could store latent heat of 153–182 kJ/kg [26]. Glauber salt has a melting temperature of 32 °C, a high latent heat of 254 kJ/kg and is an inexpensive material but shows problems with phase segregation, similar to most other hydrated salts [27].

Amongst the potential problems with using PCMs for active heating/cooling, the usually very low thermal conductivity should be mentioned [28]. To increase their thermal conductivity, metallic or graphitic nano- or microstructures can be embedded in the PCM, whereupon too much additional conductive material would reduce the specific energy storage capacity [29,30].

Depending on the environmental conditions, this range of energies stored as latent heat defines how long a PCM can maintain its melting/solidifying temperature, naturally scaling with the mass of PCM included in a garment. However, the calculation is less simple than may be expected. For a PCM inside a spherical capsule of approx. 100 mm diameter, Tan et al. compared experimental observations during melting with a computational approach [31]. They found thermally stable structures at the top of the capsule, while unstable structures were found at the bottom of the capsule, as depicted in Figure 2a, leading to clear differences in the calculated and measured temperatures, especially in the lower half of the capsule, as visible in Figure 2b [31]. Besides, calculations with different numerical simulations may lead to slightly varying results [32]. In addition, even small changes in the melting temperature near the environmental temperature will lead to large changes in the additional necessary energy to keep a defined temperature [33]. Besides the melting temperature, thermal conductivity was found to have the largest influence

on the cooling energy demand [34]. Due to these potential sources of relatively large errors, this review will concentrate on the measured effects of PCMs in garments in cold environments reported in different studies instead of extrapolating the measured findings to other environmental situations.

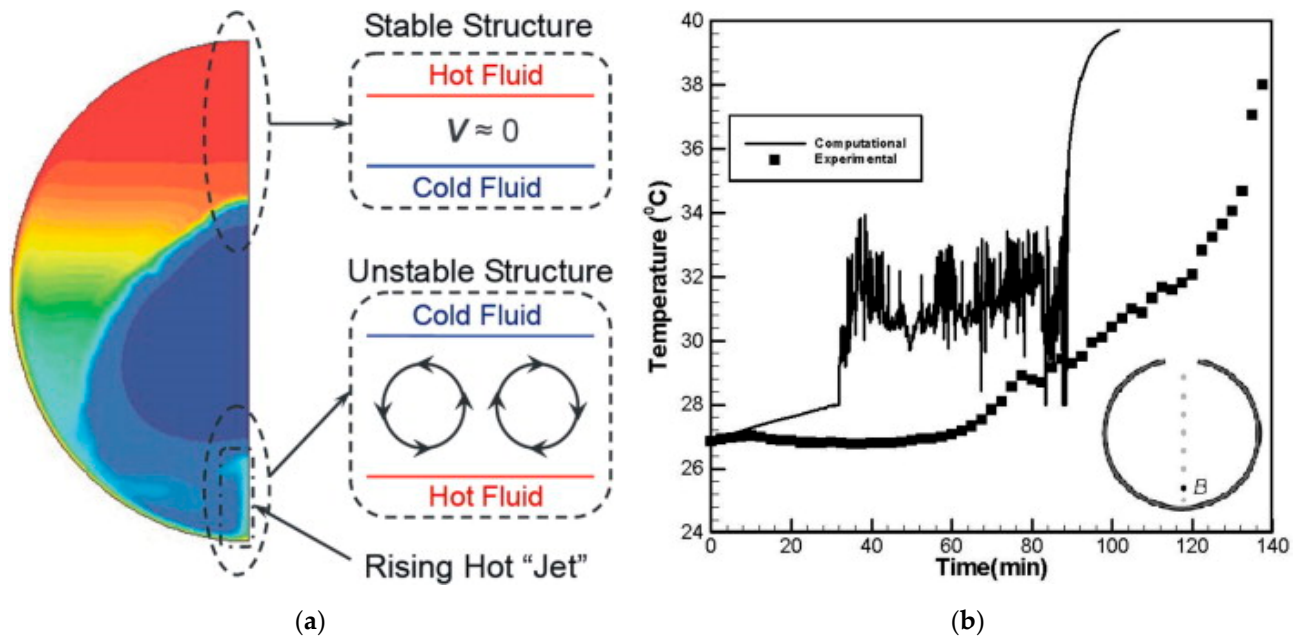


Figure 2. (a) Thermally stable and unstable layer structures along the symmetry axis; (b) comparison of the computed and measured temperatures at point B at a distance of 0.369 diameters below the center. Blue areas depict the cold, unmolten solid phase, while red areas are hot, molten liquid. Reprinted from [31], Copyright 2009, with permission from Elsevier.

2.2. Joule Heating

The most often used possibility for converting electrical energy into heat is based on the so-called Joule heating, also called resistance heating or electro-thermal conversion [35]. Theoretically, the heating power P can simply be calculated by the Joule–Lenz law as $P = RI^2 = U^2/R$, with the resistance R and the current I flowing through it. The thermal energy Q_W is equal to the electrical energy E_{el} and can be calculated as the integral over P , or in the case of time-independent power, it becomes $Q_W = E_{el} = Pt$ with the duration t of heating [17]. This means that conductive materials are necessary for electro-thermal conversion, such as intrinsically conductive polymers or polymers filled with metallic nanoparticles, graphene, graphite, carbon nanotubes, carbon black or, nowadays, MXenes [17]. For use in garments, all of them have specific challenges, such as relatively low conductivity and missing long-term stability of conducting polymers, health risks posed by metallic nanoparticles and MXenes, or low washing resistance of graphene and other materials [17]. Nevertheless, Joule heating is a very often studied method for producing clothing with active heating. It should be mentioned that while the resistance of the heating circuit in a textile fabric is essential for the heating power, this value is often not given or only partly given as linear resistance of a yarn or sheet resistance of a coating whose thickness may be different in different areas of a garment. This makes calculations of the heating power and necessary energy often complicated or even impossible.

2.3. Peltier Element Heating

Peltier elements are based on the Peltier effect, or thermoelectric effect, which converts electrical energy into a temperature gradient inside a semiconducting material [36]. Several factors influence the figure of merit, which defines the performance of organic, inorganic or hybrid Peltier materials, which should have low thermal conductivity, high electric

conductivity and a high Seebeck coefficient [37]. Due to the interconnections between these parameters, optimization is not straightforward but necessitates complicated methods such as strengthening phonon scattering [38], band engineering [39] or nanostructuring materials [40].

It must be mentioned that, unlike Joule heating textiles, Peltier elements do not heat up through the whole material but have one warmer and one cooler side. Schmidl et al., e.g., prepared Al-doped ZnO-coated polyester spacer fabrics and measured a temperature difference between both sides of the spacer fabric of up to 12 K, which was converted upon changing the polarity of the electrical contacts [41]. This fact must be taken into account when an active heating garment based on Peltier elements is created. On the other hand, Peltier elements in clothing offer heating and cooling depending on the polarity of the applied voltage, making them highly suitable for varying weather conditions [42].

3. Energy-Harvesting Textiles

While PCMs store thermal energy received from the environment in the form of latent heat, electrically heated textiles need to harvest and store energy that can be used for active heating. Mainly, such devices are based on triboelectric nanogenerators (TENGs), solar cells and thermoelectric devices [43], but there are also other mechanisms integrated into different smart textiles to harvest body heat energy, biochemical energy, etc. [44]. This section gives an overview of potential methods of harvesting energy by clothing.

3.1. Triboelectric Nanogenerator

When a person is moving, this mechanical energy can principally be harvested by a triboelectric (nano)generator (TE(N)G) [45]. Movements of the human body, such as walking or arm movements, offer several ten watts of kinetic power [46]. A TENG can be used to transfer movements into contact electrification and electrostatic induction, in this way harvesting energy from human motion [47,48]. Generally, a TENG consists of two materials with different electron affinity, resulting in electrostatic induction when these materials are coupled and moved relative to each other during body movements [49]. This induced potential difference can be reduced by a current through a load connecting the electrodes attached to the triboelectric materials, thus resulting in an AC power output for a periodic movement [49]. Depending on the positioning and movement of triboelectric materials and electrodes, TENGs can be separated into vertical contact-separation mode, lateral sliding mode, single-electrode mode and freestanding triboelectric-layer modes, as depicted in Figure 3 [49]. Most textile-based TENGs work in the vertical contact separation mode due to the ease of embedding them into shoe insoles or other textiles that are steadily pressed or stretched [49].

The first textile-based realizations of TENGs were based on coated yarns, e.g., one with carbon nanotubes and the other one with polytetrafluoroethylene (PTFE), to convert motion or vibration energy into electric energy by the electrostatic effect, leading to relatively small output power densities of ~ 1 mW/m² [50]. A similar value of 1.8 mW/m² was reported for alternating polyimide (PI)/polyurethane (PU) strips on a sleeve and alternating polydimethylsiloxane (PDMS)/aluminum strips on the torso for a movement frequency of 1.5 Hz [51]. Slightly higher power densities of 27 mW/m² were reported for a TENG that combined shear-thickening fluid and magneto-sensitive films, in this way adding impact-resistant properties [52]. A much higher power density of 953 mW/m² was found for a single-thread TENG, produced using a stainless-steel core with a silicone rubber shell and placed on a textile in a sine-like shape [53]. An approx. doubled power density of 2 W/m² was found for a PEDOT:PSS-coated textile and PTFE under foot stepping with a frequency of 2 Hz [54]. Still higher values of 3.2 W/m² were found for a freestanding triboelectric-layer TENG prepared from Ni-coated electrodes and a parylene triboelectric layer [55]. Even 8.9 W/m² was reached by a TENG in which the palm skin was used as a freestanding triboelectric layer and a silicone rubber- and Ni-coated polyester woven fabric as an electrode [56]. Developing textile-based TENGs further, an extremely high power

density of 336 W/m^2 was reported for an AlNP-coated top textile and a nanostructured PDMS bottom textile [57].

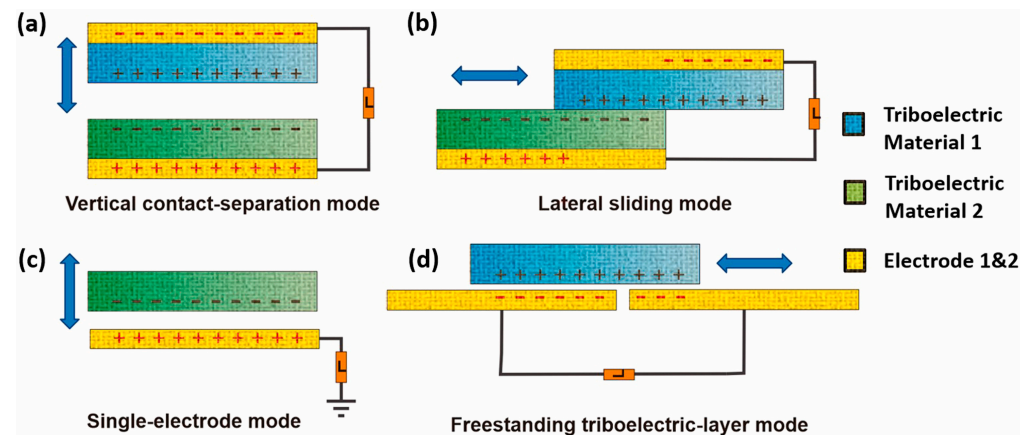


Figure 3. Fundamental modes of TENGs: (a) Vertical contact-separation mode; (b) lateral sliding mode; (c) single-electrode mode; (d) freestanding triboelectric-layer mode. Reprinted from [49], Copyright 2019, with permission from Elsevier.

It should be mentioned that these areal power densities are usually peak instantaneous values, while many applications—such as active heating—necessitate a DC power [49]. Besides, the comparison above is based on different areas, varying frequencies and different forces and loads, making a rating of recently investigated textile TENGs complicated. In addition, wash-and-wear resistance, as well as general durability, are in many cases not given, and the areal power density does not take into account the thickness or mass of the respective textile. However, power densities in the range of some ten milliwatts per square meter up to a few watts per square meter are typical for recent textile TENGs and can be used as a base for calculations of harvestable electric energies.

3.2. Solar Energy

Solar energy is the primary source of energy on Earth; thus, harvesting is a natural approach. Different photovoltaic (PV) materials are able to convert the photons of sunlight into electrical energy using the photovoltaic effect [58]. The photovoltaic conversion efficiency can be calculated as $\eta = P_{out}/P_{in}$, with the output electrical power P_{out} and the input solar radiation power P_{in} [58]. While conventional PV systems are rigid, nowadays flexible PV cells can also be produced, e.g., based on dye-sensitized solar cells (DSSCs) [59,60].

To produce photovoltaic textiles, usually flexible, organic PV films are mounted on a fabric, or textile fibers/yarns or textile layers are prepared to have photovoltaic properties [60,61]. Typical efficiencies of such textile-based solar cells are around 1% for optimum production methods, dyes—in the case of DSSCs—and conductivities of the electrodes [62–64] but can be much smaller if non-toxic materials are used for a planned application near the human body [65–67]. Assuming a conversion efficiency of 1% and a perfect orientation of the textile towards the sun, the average solar radiation flux density of approx. 165 W/m^2 [68] would enable energy harvesting of 16.5 W/m^2 with textile-based solar cells.

Generally, such textile-based solar cells are problematic to tailor, which is only scarcely addressed [69]. Wash is even more complicated and necessitates encapsulation, e.g., by lamination and thus modifying the original textile haptics, or by using very small, encapsulated modules, which only slightly increase the bending rigidity of a textile fabric [70–72]. However, these challenges, combined with the well-known problem that efficiencies are reduced for larger cells [73], typically reduce the aforementioned optimum solar energy harvesting.

3.3. Thermoelectric Devices

While Peltier elements can be used to create a temperature difference between both sides of the element by applying a voltage (cf. Section 2.3), the Seebeck effect can, vice versa, be used to generate a thermoelectric potential energy due to a temperature difference between both electrodes on the respective thermoelectric element [74]. Generally, a thermoelectric element consists of a pair of *p*- and *n*-doped semiconductors between a hot and a cold side in which the heat flow from the hot to the cold surface is accompanied by an electric current, as depicted in Figure 4 [75]. The generated voltage V is proportional to the temperature difference ΔT according to $V = \alpha \Delta T$ with the Seebeck coefficient α [75]. The power generation also depends on the cross-sectional area of the thermoelectric device and the length of their legs, besides the aforementioned material properties, such as the Seebeck coefficient and electrical and thermal conductivity [75].

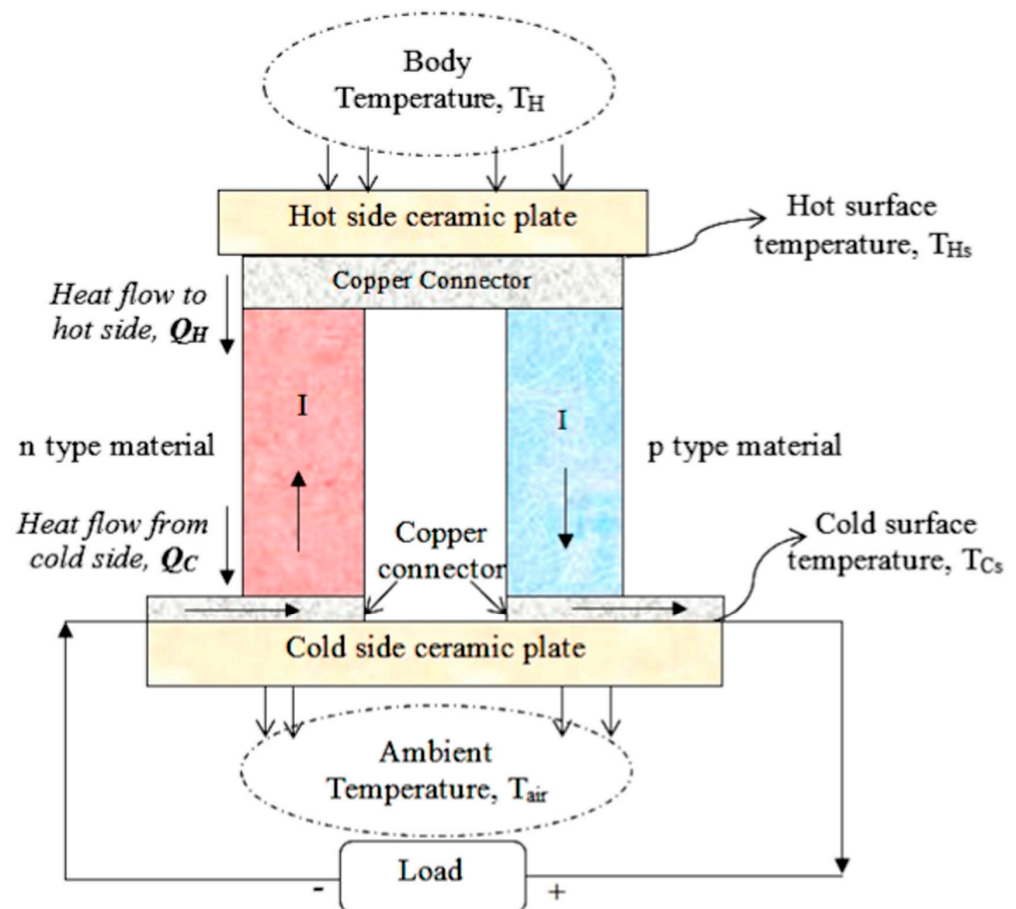


Figure 4. Single thermoelectric pair consisting of *n*-type and *p*-type materials. Heat flows from hot side to top side ($Q_H \rightarrow Q_C$), and electrical current (I) flows from *n*-type to *p*-type material due to a temperature gradient ($\Delta T = T_{Hs} - T_{Cs}$). Reprinted from [75], Copyright 2017, with permission from Elsevier.

With a wearable thermoelectric generator, calculated for a skin temperature of 34 °C, ambient temperature of 22 °C and a heat flow of 20 mW/cm², the human body could maximally generate 180 μW/cm², i.e., 1.8 W/m², with power generation around 1–37 mW for different body parts [76,77]. For larger temperature differences than 12 K, the generated energy would be accordingly higher. While this value is approx. one order of magnitude lower than the previously mentioned theoretical value for textile-based solar cells, it is similar to the range of values reported for TENGs, as discussed before.

Several researchers have investigated textile-based thermoelectric generators and optimized them. Lund et al. used a combination of PEDOT:PSS-coated silk threads and

silver-plated polyamide threads to produce a thermoelectric generator by hand-sewing through nine layers of felted wool, connected the legs on the textile surface by coating with a silver-containing paste, and measured the power generation for the hot plate at 35 °C and the cold plate at −30 °C to −5 °C, with results as depicted in Figure 5 [78]. With a device area of (5.3 cm)² and an optimized design, they reached a maximum of 1.2 μW for $\Delta T = 65$ K [78], i.e., approx. 427 μW/m² if the whole surface area is taken into account, not only the embroidered parts.

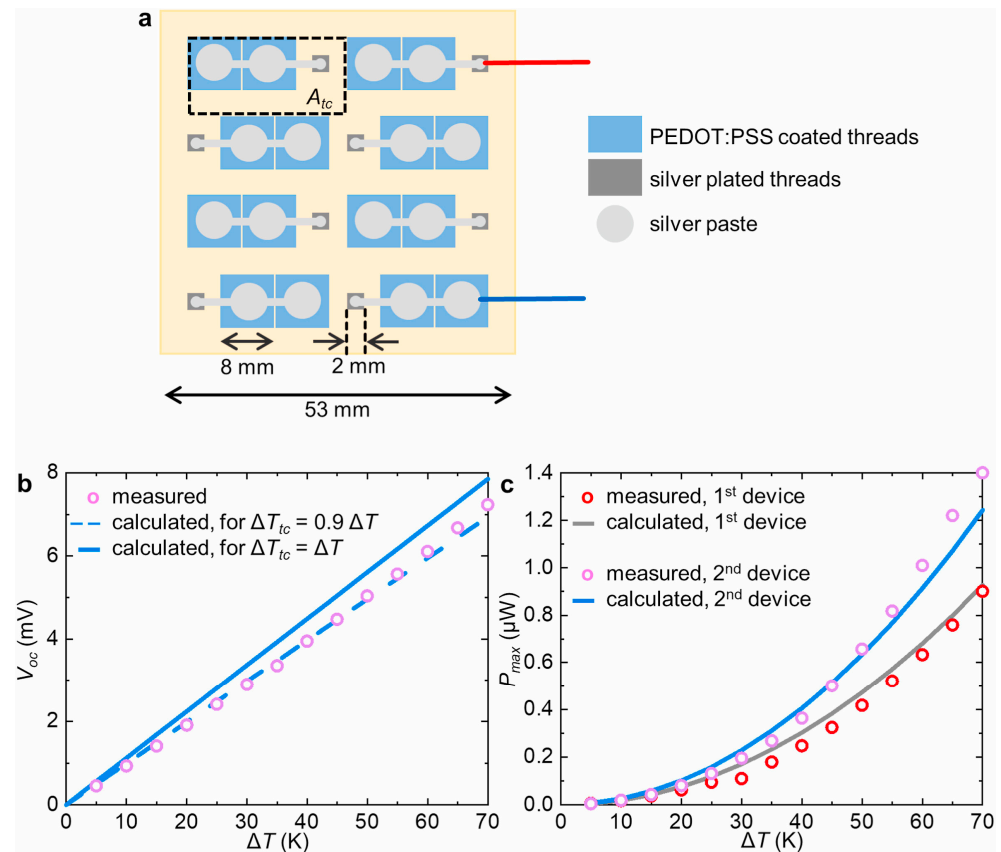


Figure 5. (a) Schematic of optimized textile thermopile with optimized leg areas, red and blue lines are connectors to the voltage measuring equipment. (b) Measured open-circuit voltage V_{oc} (circles) as a function of the temperature gradient ΔT between the hot plate and the cooler, and calculated data for V_{oc} as a function of ΔT , where $\Delta T_{tc} = \Delta T$ (solid line) and $\Delta T_{tc} = 0.9 \cdot \Delta T$ (dashed line). (c) Measured generated power (circles, red for the 1st thermopile, purple for the 2nd thermopile) as a function of ΔT and calculated generated power (solid lines, grey for the 1st thermopile, blue for the 2nd thermopile) assuming $\Delta T_{tc} = 0.9 \cdot \Delta T$ and electrical contact resistance of 1.2 Ω (1st thermopile) or 1.1 Ω (2nd thermopile) per thermocouple. Reprinted from [78], originally published under a CC-BY license.

With 864 connected legs coated with PEDOT:PSS and poly([Na(NiETT)]), respectively, on an area of (25 cm)², a temperature difference of 3 K resulted in a power of 13 μW, whereupon the authors calculated that densely filling 8% of the whole body surface area with the legs of a thermoelectric generator would result in 1 mW power output [79]. Combining PEDOT:PSS and a *p*-type semiconductor with *n*-type Ag₂Te, a power output of 6 mW/m² was reached by a temperature difference of 20 K [80], while Ag₂Se with Ag connection resulted in a power density of 2.3 W/m² for $\Delta T = 30$ K [81].

For a one-dimensional thermoelectric generator with PEDOT:PSS and carbon nanotube/polyethylenimine hydrogel fibers, a value of 4.8 W/m² was found for a temperature difference of 60 K [82]. On the other hand, a three-dimensional woven textile produced from a yarn with alternating *n*- and *p*-type segments reached a power output of approx. 0.65 W/m² for a typical temperature difference of 55 K [83]. In many cases, however, only

a maximum power is given for a textile-based thermoelectric generator [84], making it more complicated to estimate the maximum thermoelectric power that could be generated by garments.

3.4. Other Energy Harvesting Methods

Among the other methods of energy harvesting by garments, piezoelectric textiles must be mentioned, which are regularly investigated. As depicted in Figure 6, piezoelectric materials perform a charge separation when a pressure is applied or released, leading to a voltage [85]. Amongst the possible materials that show the piezoelectric effect, such as ZnO, BaTiO₃ or GaPO₄, especially polyvinylidene fluoride (PVDF) has often been investigated due to its good mechanical properties, flexibility and chemical and thermal stability [85–87]. For this material, Liu et al. reported an efficiency of around 12% for the transition of mechanical into electrical energy and vice versa [88]. With a combination of PVDF, BaTiO₃ nanoparticles and reduced graphene oxide nanoplates, even an energy conversion efficiency of 22.5% was reached [89]. For single melt-spun PVDF, polyamide 11 and polypropylene fibers, powers in the range of 0.2 nW were generated [90]. Combining PVDF with lead zirconate titanate (PZT), a piezoelectric nanogenerator from electrospun-aligned nanofibers produced 6.35 μ W [91]. Besides electrospinning and melt spinning as typical fiber production methods, it is also possible to use physical or electrochemical deposition of piezoelectric materials on textile fabrics, which is especially relevant for non-polymeric materials such as ZnO [58].

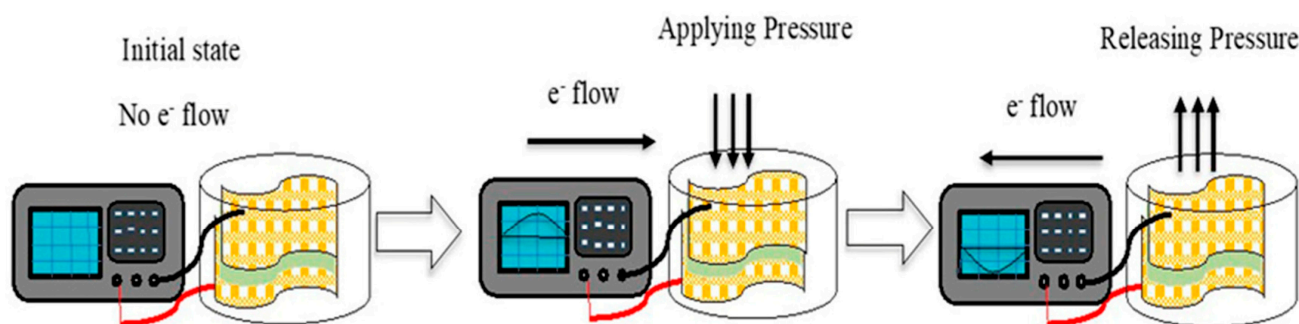


Figure 6. Working principle of a piezoelectric material when applying and releasing pressure. Reprinted from [85], originally published under a CC-BY license.

Other research groups suggested additional methods of harvesting energy by smart textiles, e.g., biological fuel cells that generate energy by biodegradation of organic matter [92,93], partly using the wearer’s sweat to harvest biochemical energy [94].

Generally, as suggested by Lund et al. [78], a reasonable combination of different energy harvesting methods should be applied to optimize the overall gained energy. Depending on the environmental conditions (temperature difference, sunlight) and movements of the person wearing the respective harvesting garments, a power density of the order of magnitude 1 W/m² can be expected. In the next section, storing the energy harvested in a defined time in textiles will be discussed.

4. Energy-Storing Smart Textiles

Most of the aforementioned forms of energy that can be transferred into electrical energy—sunlight, body movements—are not constantly available; only the temperature difference between skin temperature and surrounding temperature, as used in thermoelectric devices, is automatically larger when more heating energy is needed. Using a combination of different energy harvesting methods, however, necessitates storing parts of the energy harvested in sunlight and during active movements for times when it is more needed.

Several researchers thus investigated methods to store energy in textile fabrics, either fiber-, yarn- or fabric-based, usually in the form of batteries or supercapacitors, as depicted in Figure 7 [95].

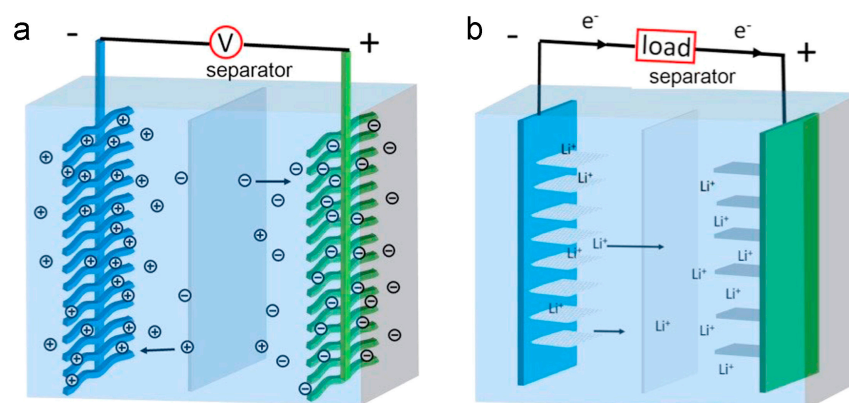


Figure 7. Schematic illustrations of energy storage mechanisms of (a) a supercapacitor and (b) a lithium-ion battery. Reprinted from [95], Copyright 2016, with permission from Elsevier.

In all these cases, several design strategies have to be taken into account, such as flexibility and washability of the materials, but also the electrical conductivity of electrodes and wires, as well as more specific physical and chemical properties of the materials used for batteries or supercapacitors [95–97]. This section discusses recent approaches to storing electrical energy in textile fabrics.

4.1. Fiber-Based Supercapacitors

Fiber-based supercapacitors can be produced, e.g., by wet spinning, dry spinning, microfluidic spinning, hydrothermal self-assembly and other methods based on graphene and other materials [98]. An example of the production of a fiber-based supercapacitor is shown in Figure 8, based on nitrogen-doped SiNs/graphene hybrid fibers [99]. More precisely, the exfoliation of CaSi_2 using HCl resulted in siloxene (SiNs) nanosheets after several days, which were coated with polypyrrole (Ppy) before these nanosheets were pyrolyzed, resulting in a nitrogen-doped carbon layer on the siloxene nanosheet (N-SiNs) (Figure 8a). Wet spinning from a N-SiNs/GO (graphene oxide) dispersion and chemically reducing the GO into rGO (reduced graphene oxide) resulted in fiber-based supercapacitors (Figure 8b) with an areal specific capacitance of 264 mF/cm^2 [99]. The capacitance C of a supercapacitor enables storing an energy of $E = 1/2CV^2$ with voltage V .

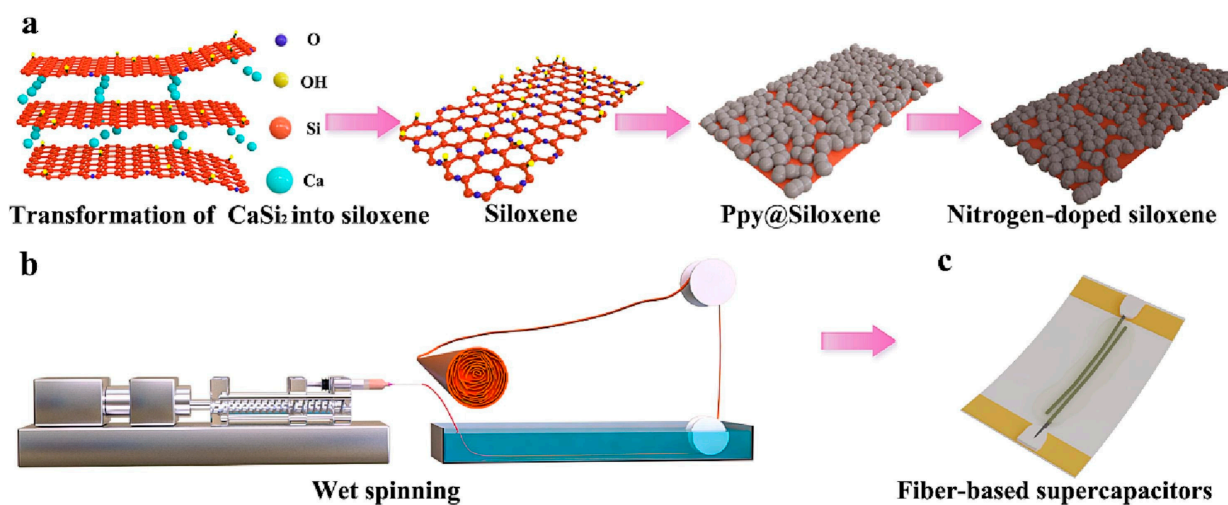


Figure 8. Schematic illustration of the fabrication of the N-SiGF sample and the fiber-based supercapacitors (a–c). Reprinted from [99], Copyright 2023, with permission from Elsevier.

When comparing different supercapacitors, it must be taken into account that sometimes only the electrodes are taken into account when calculating the capacitance for a

certain mass, volume or area, while in other studies, the whole supercapacitor, including the separator and the electrolyte, is considered [100]. On the other hand, sometimes, the power density is given instead of an energy density.

A fiber-shaped supercapacitor in the form of a partially unzipped carbon nanotube/rGO hybrid fiber was produced by wet spinning and chemical reduction, leading to a high volumetric energy density of 8.63 mWh/cm^3 [101]. For an alginate/PEDOT:PSS@Ppy composite fiber, a volumetric capacity of 568 F/cm^3 and an areal capacity of 1000 mF/cm^2 were found, as well as a high energy density of $21 \text{ } \mu\text{Wh/cm}^2$ [102]. A smaller areal capacitance of 115 mF/cm^2 and a similar energy density of $9 \text{ } \mu\text{Wh/cm}^2$, as well as a power density of 0.11 mW/cm^2 , were reported for hollow PEDOT:PSS thin-walled fibers [103]. Nanostructured MnO_2 -based fiber-in-tube and particle-in-tube supercapacitors reached a capacity of 432 F/g , an energy density of 46 mWh/g and a power density of 400 mW/g [104]. Combining activated carbon fiber as substrate and a polyaniline (PAni) composite fiber coated with commercial pen ink resulted in a linear capacitance of 108 mF/cm or 68 mF/cm^2 , which was coupled with MnO_2 @ink/activated carbon fiber to reach an energy density of $102 \text{ } \mu\text{Wh/cm}^2$ and a power density of 1 mW/cm^2 [105]. A capacitance of 17.5 F/cm^3 or 10.7 F/g , leading to an energy density of 7.88 mWh/cm^3 or 4.82 mWh/g and a power density of 2.26 W/cm^3 or 1.382 W/g , was reported for an asymmetric supercapacitor, produced by twisting a MnO_2 /CNT fiber cathode and a Ppy/CNT fiber anode combined with a LiCl/poly(vinyl alcohol) (PVA) electrolyte [106].

An interesting approach based on jute fibers with PEDOT:PSS and single-wall CNTs, combined with a cellulose-based material as separator, was shown to reach an energy density of $0.71 \text{ } \mu\text{Wh/cm}^2$ and a power density of $3.85 \text{ } \mu\text{W/cm}^2$, as well as a specific capacitance of 8.65 mF/cm , which is much smaller than the aforementioned values but was aiming at a more environmentally friendly approach [107].

To evaluate these different values, we can assume that the power gained with the aforementioned energy-harvesting textiles, which is in the order of magnitude 1 W/m^2 , should typically be stored for approx. half a day, e.g., due to harvesting sun and movement energy during daytime and releasing it again during nighttime, so that an energy of the order of magnitude 10 Wh/m^2 should be stored if the whole textile area covering the human body is used for energy harvesting as well as for energy storing. The energy densities reported for fiber-based supercapacitors are typically in the range of 5 mWh/m^2 – 1 Wh/m^2 , comparing the aforementioned and other values [108], which would not be sufficient to store the whole energy that can theoretically be gained during half a day. However, there are a few reports mentioning one or two orders of magnitude higher energy density, such as 147 Wh/m^2 for a core-shell MoS_2 nanosheet array/graphene hybrid fibers showing an increased specific capacitance by two orders of magnitude due to the MoS_2 nanosheet array surface deposition [109]. Apparently, it is necessary to use such specific materials to enable storing all possibly harvested energy for about a half day in fiber-based supercapacitors.

4.2. Fabric-Based Supercapacitors

Fabric-based supercapacitors can be produced by different coating, printing and lamination methods. As an example, for an inkjet-printed MnO_2 - NiCo_2O_4 /rGO (positive/negative electrode) asymmetric supercapacitor on bamboo fabric, an areal capacitance of 2.12 F/cm^2 was found, leading to an energy density of 37.8 mWh/cm^3 and a power density of 2.7 W/cm^3 [110]. For a supercapacitor based on carbon fiber electrodes functionalized with vertical graphene and MnO_2 and a glass fiber separator, Sha et al. reported an areal capacitance of 31 mF/cm^2 , an energy density of 12 mWh/kg and a power density of 2210 mW/kg [111]. Wen et al. showed a flexible zinc-ion supercapacitor with an energy density of 0.32 mWh/cm^2 , which could also be used as a strain sensor [112]. A detailed overview of materials, production methods and energy densities of fabric-based supercapacitors can be found in [113] (Figure 9).

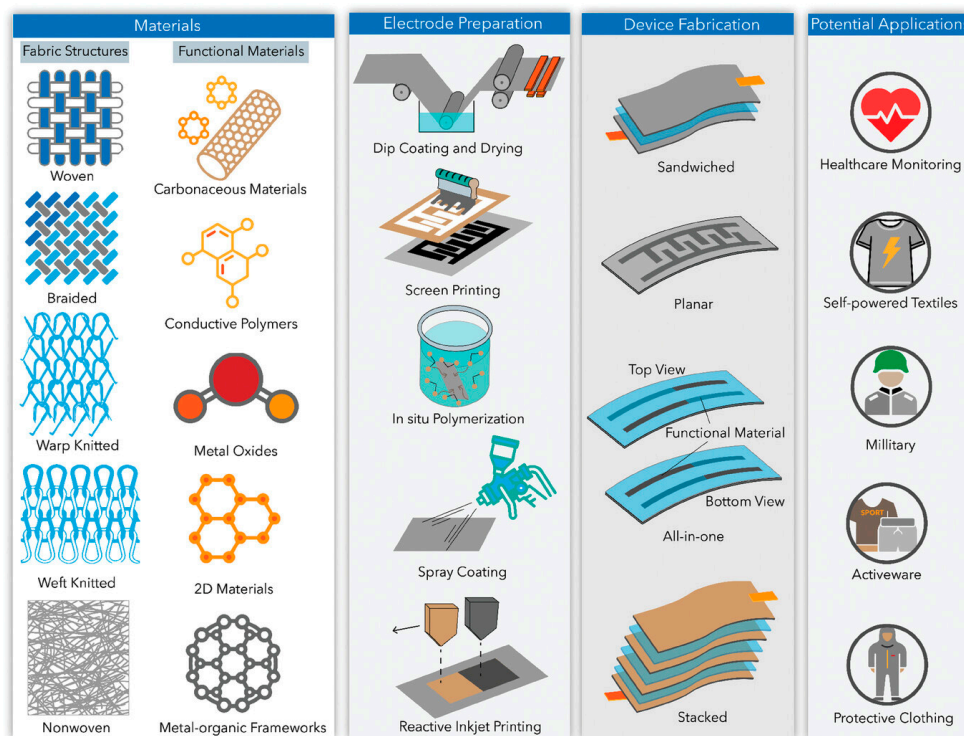


Figure 9. Materials, preparation methods and potential applications of fabric-based supercapacitors. From [113], originally published under a CC-BY license.

In his recent overview, Khadem [113] reported energy densities of up to 4.7 Wh/cm^2 , i.e., 47 kWh/m^2 [114], which would be more than sufficient to store the aforementioned 10 Wh/m^2 energy for approx. half a day of energy harvesting, or even 190 kW/m^2 [115] or 1.5 MWh/m^2 [116]. However, most energy densities are several orders of magnitude smaller [113,117–120], so here again, it is important to properly choose a suitable fabric-based supercapacitor to enable sufficient energy storage capacity.

4.3. Flexible Batteries

Flexible fiber- or fabric-based batteries, such as lithium- or zinc-based batteries, often suffer from problems regarding encapsulation, high internal resistance and low durability [121]. There are, however, many more anode and cathode materials that have been investigated for their potential use in flexible batteries, such as carbon, titanium compounds, chalcogens or Na as anode materials and different oxides, sulfur or gasses as cathodes, combined with different aqueous, gel-polymer or solid-polymer electrolytes, several of which have also been investigated for fiber- or fabric-based batteries [122]. Recently, other potential electrode materials, such as vanadium nitride, have been suggested [123].

A solid-state Zn/MnO₂ fiber battery with high cycling stability was suggested by Xiao et al., who used a graphene oxide (GO)-embedded polyvinyl alcohol (PVA) hydrogel electrolyte (GPHE) (Figure 10) [124]. They found good mechanical properties, such as a stretchability of 230% without breakdown and self-healing of the gel electrolyte, as well as an energy density of 91 Wh/L , i.e., 91 mWh/cm^3 [124]. For a highly elastic fiber-based graphene/PAni-Zn@silver battery with a helical structure, a capacitance of 32.6 mAh/cm^3 and an energy density of 36 mWh/cm^3 were reported [125].

For fabric-based batteries, other problems may occur due to fractures of metalized areas [126]. Printed batteries, e.g., by screen printing or inkjet printing, are thus advantageous for the production of flexible fabric-based batteries [127]. Alternatively, batteries can be produced as (nano-)composites from fibrous materials, as depicted in Figure 11 [128]. The fabric-based battery depicted here, based on NiCo₂S₄@rGO nanocomposites, reached a power density of 3.2 W/g and an energy density of 0.455 Wh/g [128]. A similar energy

density of 0.429 Wh/g was found for a sodium-ion with $\text{Na}_3\text{V}_2(\text{PO}_4)_2\text{F}_3@\text{C}$ cathode [129]. For a potassium-ion battery with potassium nickel iron hexacyanoferrate as the cathode material, an energy density of 0.283 Wh/g was reported [130].

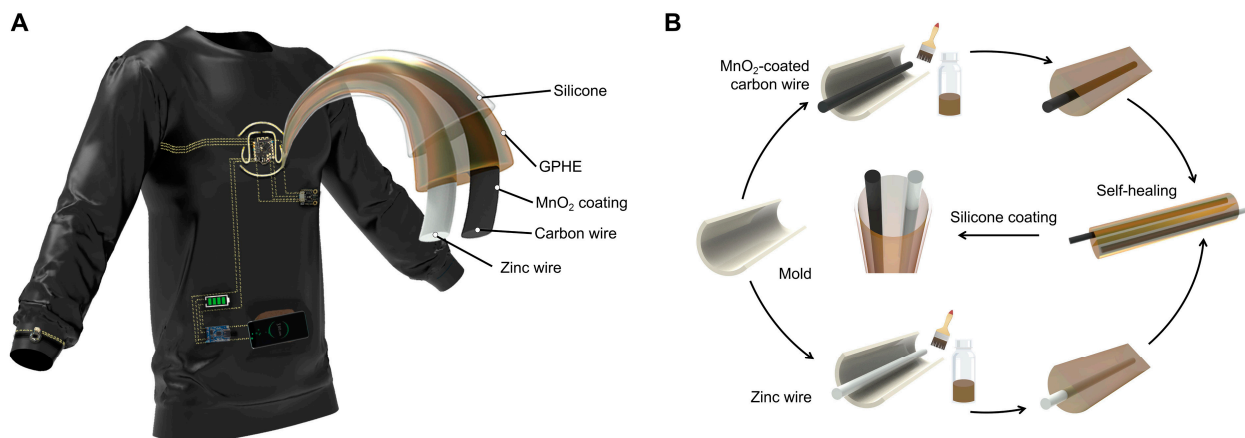


Figure 10. (A) Illustration and design of a flexible zinc-ion battery textile body area network. (B) Fabrication process of the functional fibers as the building blocks. From [124], originally published under a CC-BY-NC license.

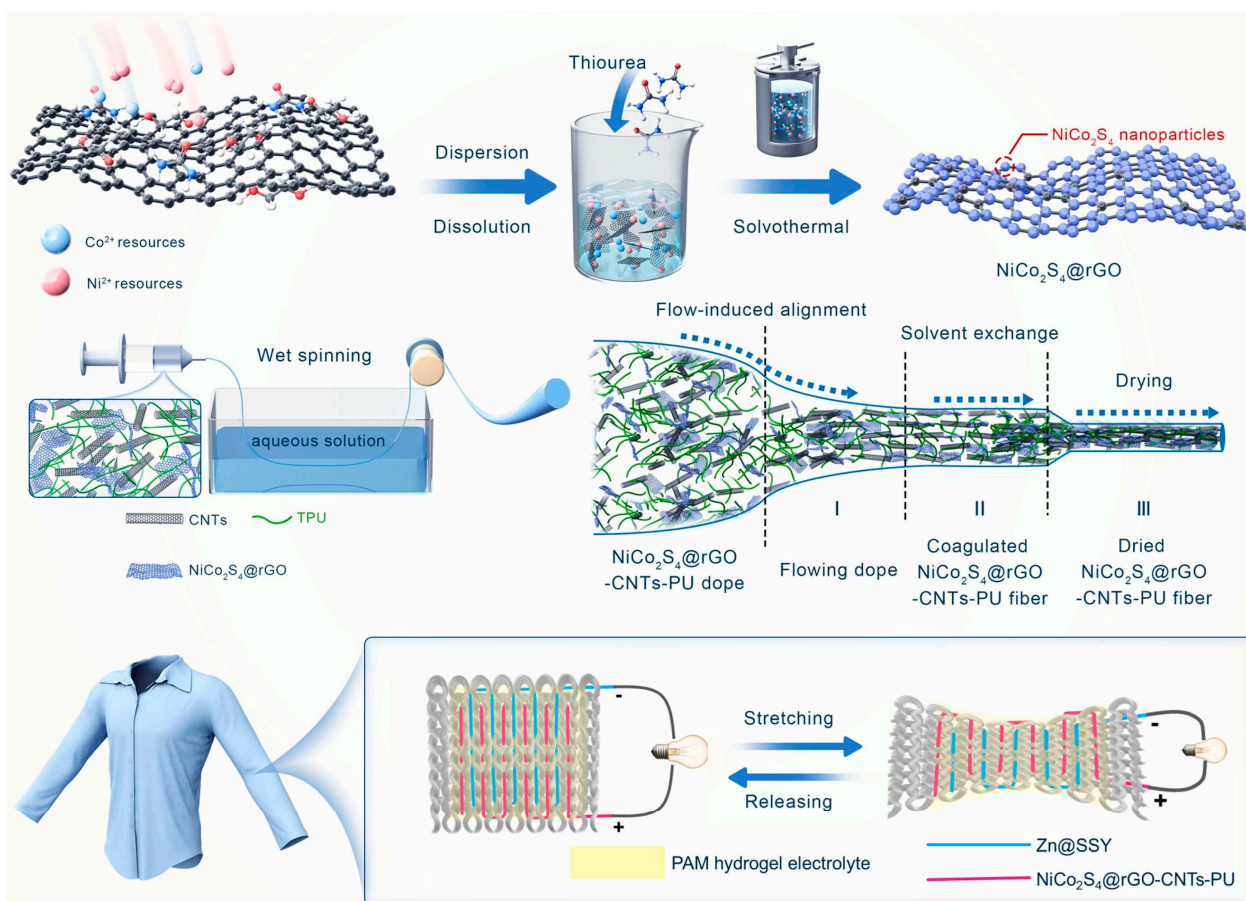


Figure 11. Schematic illustration of the fabrication of $\text{NiCo}_2\text{S}_4@\text{rGO}$ nanocomposites, $\text{NiCo}_2\text{S}_4@\text{rGO}$ -PU-CNTs fiber cathodes and serpentine footprint fabric Zn-based batteries. PAM: polyacrylamide, CNT: carbon nanotube, PU: polyurethane, rGO: reduced graphene oxide. Reprinted from [128], Copyright 2024, with permission from Elsevier.

For a broad range of different flexible batteries, either fiber- or fabric-based, Wang et al. reported areal energy densities around 6–60 Wh/m² for flexible lithium-ion batteries, 1–20 Wh/m² for sodium-ion batteries, and 1.5–62 Wh/m² for zinc-ion batteries [131]. On the one hand, these values do not differ as strongly as those for fiber- or fabric-based supercapacitors, making batteries potentially easier to build than flexible supercapacitors. On the other hand, the aforementioned value of 10 Wh/m², as a typical order of magnitude which energy could be harvested during half a day by textile fabrics, can be reached by all of these typical fiber- or fabric-based batteries.

As this section showed, it is thus generally possible to store the energy that could be harvested in half a day inside a textile fabric of the same area, e.g., directly below a photovoltaic textile. On the other hand, it is still necessary to find out which heating energy is necessary in different situations, either for short stays in very cold environments, such as space or cold stores, or for longer durations outside in the winter. The next section will discuss active heating by electric energy or by PCMs, where the latter will be regarded with respect to the duration of melting or crystallization at defined temperatures, while the first will be discussed in terms of necessary electric energy.

5. Energy-Self-Sufficient Heating Textiles

Some research groups have investigated energy-self-sufficient—or self-powered—heating textiles. In many cases, these studies are based on PCMs that can store a defined amount of energy and release it afterward when the environmental temperature is reduced.

5.1. PCM as Self-Sufficient Heating Textiles

To get an idea of the energy that should be stored in PCMs, it is supportive to use the heat that can be produced by a person, which is about 100 W at rest to about 600 W or even more during work or sports [132]. Typical values of heat storage capacity of phase-change materials are in the order of magnitude 200 J/g [132], meaning that energy of 1 kWh, as released by the human body at rest within ten hours, necessitates 3.6 MJ of storage capacity, i.e., phase-change material with a mass around 18 kg. This shows that PCMs from common materials, such as octadecane, hexadecane, etc., should be used more for repeatedly varying temperatures, as is the case for spacesuits in many situations, while PCMs with much higher storage capacity would be needed to support homeless people during nighttime.

It must be mentioned that there are several studies aimed at increasing the heat storage capacity of PCMs; however, for use in textile fibers or fabrics, usually an encapsulation in the form of microcapsules or core-shell fibers is needed, which reduces the mass-related heat storage capacity again. For microencapsulated PCMs with a polyurethane (PU) binder, e.g., a heat storage capacity of 0.2–7.6 J/g was reported [133].

On the other hand, the above calculation can only approximate an order of magnitude necessary to use PCMs in textiles for active heating since the necessary amount of stored energy depends strongly on the environmental temperature, isolation properties of the whole garments, activity of the wearer, etc. Additionally, thermoregulation depends on the position where the PCMs were integrated into the fabric, on the fabric construction, etc. [134]. This section thus searches for examples of measured or calculated heat retention by textile PCMs.

As an example, Zhang et al. developed a coaxially electrospun multicore-sheath nanofiber mat based on methacrylic acid (MAA), ethylene glycol dimethacrylate (EGDMA) and benzoyl peroxide (BPO) with dodecanol as a PCM, which reached a maximum latent heat value of 106 J/g [135]. Their material showed a suitable phase-change temperature of around 25–30 °C, latent heat retention of more than 98.3% after 500 thermal cycles, and nearly unchanged latent heat and tensile strength after soaking the nanofiber mat in water. The authors suggested it for potential use in space suits. Depending on the injection speed ratio of the PCM core and acrylate copolymeric shell during coaxial electrospinning, four different samples were prepared. Figure 12 shows the time-dependent temperature

development of pure polyacrylate and the core-shell nanofiber mats (with an increasing amount of PCM for increasing numbers CS-1 to CS-4) after cooling the samples from 50 °C to room temperature [135]. While a clear difference from CS-1 to CS-4 is visible, it must be mentioned that the time scale used here is not sufficient to provide active warming for a longer duration. The specimens are reported to have a thickness of 85 µm, naturally leading to fast cooling when they are placed on a table at room temperature, with much higher mass and unknown thermal conductivity. Thus, these experiments can only serve as basic material comparisons but do not allow a statement about their applicability for longer active heating in garments.

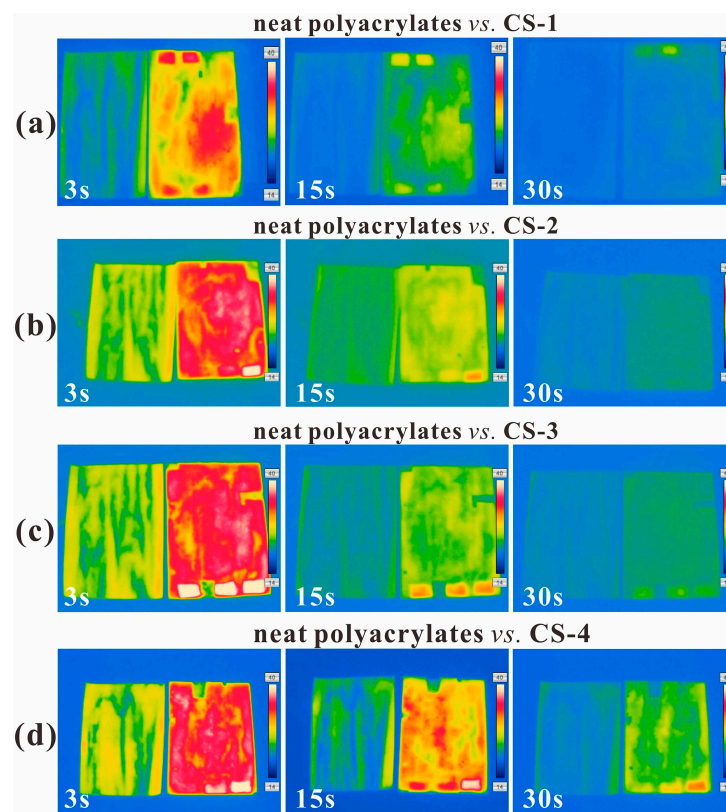


Figure 12. Thermographic images of neat polyacrylates and CS specimens after cooling from 50 °C to RT and maintaining at RT for 3 s, 15 s or 30 s. In each image, the left and the right photo, respectively, correspond to neat polyacrylates and CS specimens ((a) CS-1, (b) CS-2, (c) CS-3 and (d) CS-4). All color scales are from 14 to 40 °C. Reprinted from [135], Copyright 2022, with permission from Elsevier.

On a longer time scale of up to 60 min, Yan et al. investigated knitted fabrics, partly including hollow polypropylene (PP) fibers filled with up to 83% poly(ethylene glycol) (PEG) as the PCM [136]. The phase-change temperatures were in the range of 16–40 °C, depending on the amount of PEG in the PP fibers. Heating the samples fixed on a custom-designed sample holder up to 40 °C for 20 min by an infrared lamp and subsequently measuring the temperature of the sample with an infrared camera led to an increase in the duration that the samples needed to reach ambient temperature, from 44 min to 62 min. While this increase shows the effect of the PCM, Figure 13 [136] reveals that the difference between both investigated samples is actually not large. Besides, the inset photographs of the original and the final state show that the custom-made sample holder (of unknown material and mass) has also been heated up by the infrared lamp and is, naturally, also cooling down during the time of the experiment. Here again, the influence of the thermal contact with the unknown sample holder cannot be estimated, so the results of this study cannot be transferred to the situation of heating a person's skin in a cold environment. Generally, measuring heat retention by PCM textiles is challenging due to unclear or

non-standardized factors that vary from one study to the other, such as environmental conditions (room temperature, relative humidity, underground on which the fabric is placed during measurements), fabric construction, fabric material, mass ratio of PCM to textile fabric, etc.

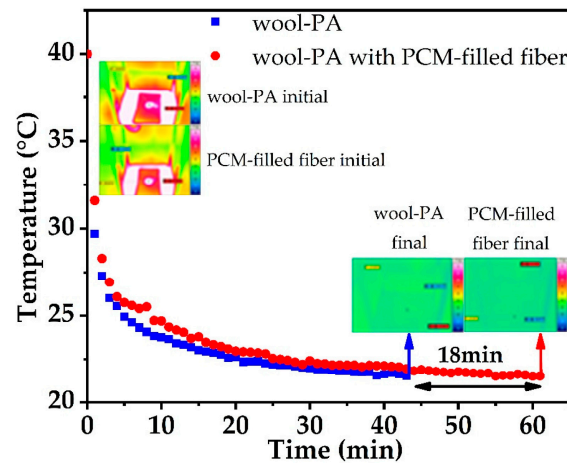


Figure 13. Temperature gradation curves of knitted wool-PA fabric with and without PEG1000-filled PP fibers. Reprinted from [136], originally published under a CC-BY license.

For the aforementioned microencapsulated PCMs with PU binder, heating durations of up to 15 min were reported in different studies [137,138]. Similarly, Ying et al. found the temperature changes between a non-PCM fabric and PCM fabrics with different PCM levels between 20 and 120 g/m², upon heating from 23 °C to 35 °C, vanished after less than 10 min [139]. Similar durations were found for a PCM-based cooling vest using Glauber's salt or pure gallium as the PCM in a heated chamber at 30–32 °C, starting from 22 to 25 °C [140].

Ghali et al. simulated the effect of a PCM textile upon a sudden change in the environmental temperature and found a heating effect for approx. 12.5 min, depending on the cold outdoor conditions, as well as a decrease of the clothed-body heat loss by 40–55 W/m² for a one-layer garment [141]. Besides oscillating temperatures, they also tested steady-state environmental conditions and stated clearly that the PCM did not influence the thermal resistance in this scenario.

Comparing the aforementioned and several other studies from the recent literature leads to the conclusion that, as discussed at the beginning of this section, PCM textiles are not suitable for long-term use at the moment but are supportive in oscillating temperatures. In addition, while only a few studies have investigated the long-term thermal performance of PCMs, the thermal characteristics of several materials were found to be unstable. Behzadi and Farid reported that Rubitherm 21, a paraffin mixture, significantly changed the peak melting point and the latent heat of fusion, while mixed esters showed nearly no such change [142]. For PCM heat storage as part of a solar combi system in a house, Johansen et al. tested sodium acetate trihydrate and found it to work properly during half a year of testing, with heating it up to 80 °C 53 times by the solar collectors [143]. For the numerical investigation of a solar greenhouse, Chen and Zhou differentiated between short- and long-term PCM storage, where an organic PCM was responsible for short-term energy storage and release during the night while no longer working in the early morning, when a mixture of salt hydrates with different melting temperatures could provide the additional long-term heating [144]. In this study, the potential change in organic and inorganic PCMs with longer use times was not investigated. Long-term stability was, however, found for TiO₂/tetradecanoic acid-based composite PCMs [145] or LiNO₃/KCl-expanded graphite (EG) composite PCMs [146]. Especially for textile fabrics, long-term stability was found for microcapsules loaded with *n*-docosane as the PCM [147].

While some tests of the long-term stability of PCMs have indeed been performed, as these examples show, the studies indicating energy storage for several hours [144] or even days [141] are still scarce and are usually not related to textile fabrics, where typically only relatively small masses of PCMs can be integrated, making them more suitable for short-term temperature variations than for energy storage for approx. half a day. The next sections will thus concentrate on fabrics heated by electric energy.

5.2. Self-Sufficient Joule Heating Textiles

Many research groups show the results of Joule heating textiles prepared in diverse ways. As an example, Ding et al. developed a polyester/spandex blend fabric-based Joule heater by coating it with CNT/polydopamine (PDA) [148]. Depending on the applied voltage, they reached different temperatures within approx. one minute, as depicted in Figure 14, where the measurements were not taken on a glove but on a not-defined underground with unclear thermal contact and unclear room temperature. Heating with voltages around 3–7 V should be sufficient for most environmental situations; however, without the resistance of the heating ring (which is not given in [148]), the calculation of a heating power or the energy necessary for longer heating is not possible.

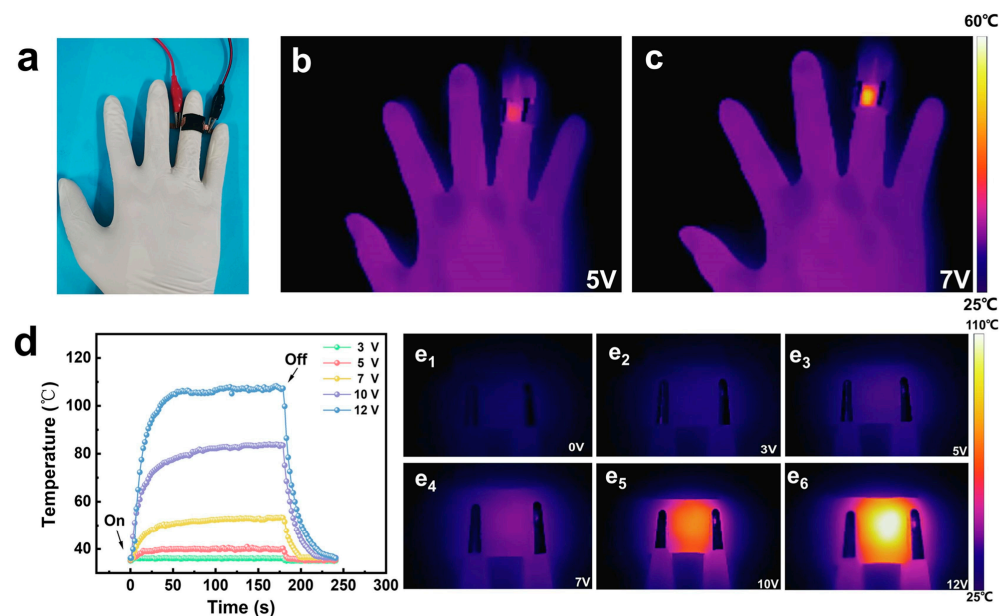


Figure 14. (a) Optical photograph of active heating textile wrapped around a finger; thermal infrared images at (b) 5 V and (c) 7 V; (d) temperature profiles of active heating textile at 3–12 V; (e₁–e₆) corresponding thermal infrared images at 0–12 V. Reprinted from [148], Copyright 2023, with permission from Elsevier.

For a cotton/tannic acid/Ag nanoparticle/PDMS knitted textile of dimensions 2 cm × 1 cm and a resistance of approx. 3.8 Ω/cm, Guo et al. reported saturation temperatures of 36–74 °C for voltages of 0.5–1.5 V, reached at a room temperature of around 30 °C [149]. This corresponds to a heating power of 0.07–0.6 W for the mentioned area of 2 cm², i.e., a necessary power density of 350–3000 W/m². It must be mentioned that this calculation highly overestimates the necessary energy for the given temperatures as the textile also has to heat the (unknown) underground, and no isolation from the environment is given, so this calculation cannot really be transferred to the situation of heating a human body in a cold environment in addition to common isolation clothing.

Many other groups also measured the temperature development of a Joule heated textile on an unknown underground instead of on a clothed thermal manikin or even on probands [150–152], making comparisons with other studies or even extrapolating to a real human in a cold environment quite challenging. This problem is also discussed in [8],

where the authors mention the problems of transferring improvements of single thermal properties, such as thermal conductivity, towards the real warming effect for the human body and mention the necessity to perform manikin tests in simulated or real environments as well as opinion polls. Shuvo et al. also discuss the influence of characterization methods of Joule heating efficiency and boundary conditions in detail [153]. Comparing the heating efficiency of different textiles with air flow to maintain a temperature of approx. 42 °C, they found necessary power densities around 230–950 W/m², which are all values far above the values estimated for the power density of typical textile energy harvesting and storage methods.

One of the few studies on human probands was reported by Song et al., who measured the skin temperature on the feet inside a conventional and a heated sleeping bag on each of seven male and female volunteers [154]. The heating pads from carbon heating wires between two high-density polyester layers of area (38 cm²) could be heated by 0–45 W, where 20 W was mostly regarded as thermo-neutral. The tests were performed in a climate chamber with air temperature −0.4 °C (for female volunteers) and −6.4 °C (for male volunteers), respectively, at an air velocity of (0.5 ± 0.1) m/s and a relative humidity of (80 ± 5)%. In all cases, a strong difference was visible for the measured temperature of the fourth toe and the left foot during 3 h of measuring, starting from approx. 24 °C (toe temperature) and nearly 30 °C (left toe) and decreasing strongly in the toe and also visibly in the foot for the conventional (unheated) sleeping bag, while the temperature slightly increased up to an approximately constant value for the heated sleeping bag, as depicted in Figure 15 [154]. Comparing the here-used heating power of 20 W with the aforementioned order of magnitude of 10 Wh/m² that could be harvested during half a day, however, shows that with an assumed garment surface of 2 m², only 1 h of using the heating pads would be possible. On the other hand, Figure 15 clearly shows that a smaller heating power would be sufficient to maintain a stable temperature of the feet.

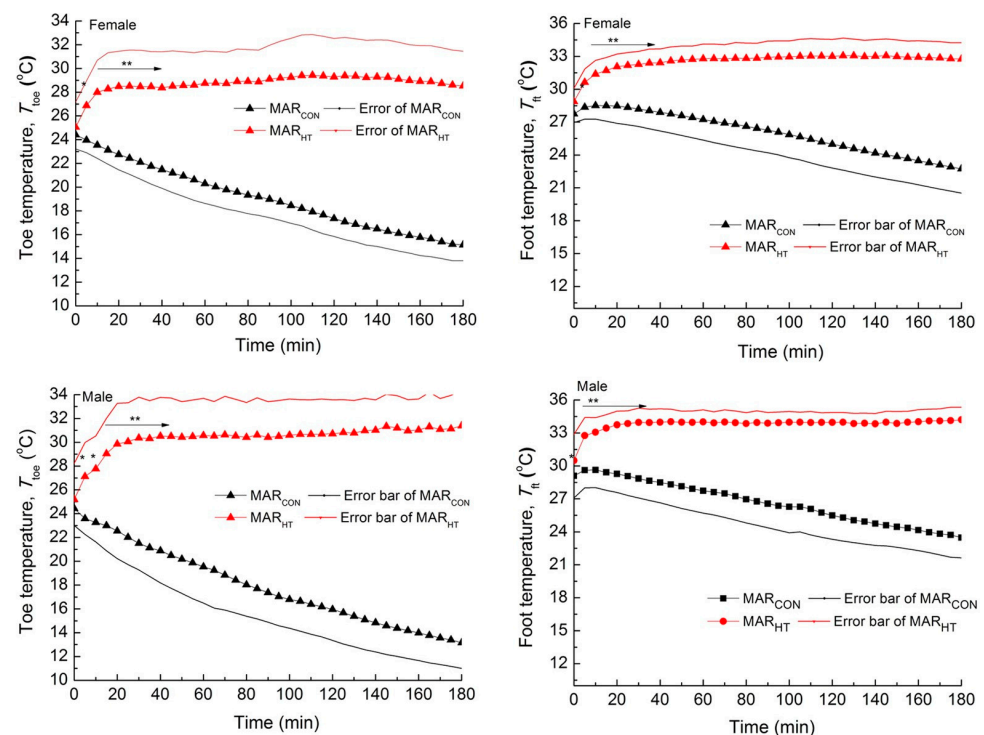


Figure 15. Evolution curves of the 4th toe and the left foot temperatures for females and males in mummy-shaped sleeping bags (conventional: MAR_{CON}, heated: MAR_{HT}). Significant deviations calculated by two-way ANOVA tests are given with significance levels $p < 0.05$ (marked * on the graphs) and < 0.01 (**), respectively. From [154], originally published under a CC-BY license.

A heated glove was used to maintain a minimum temperature of the finger surface of 15.6 °C, which had been defined as the minimum standard of spacesuit ergonomics design previously, while the environmental temperature around the clothed thermal hand manikin was −130 °C [155]. While the special extravehicular activity (EVA) glove could maintain the temperature measured at the middle finger at 20 °C for about an hour, heating was necessary after 75 min. The authors reported a heating power of 4 W to be ideal for maintaining the defined temperature of 15.6 °C [155], suggesting that either regular warming in a space vehicle or regularly taking new power supplies from the space vehicle is necessary, especially since not only the hands should be warmed during longer work in space.

Many other studies lack exact definitions and descriptions, in this way impeding extrapolations from the investigated situations to other environmental conditions. The same problem occurs for textiles heated by Peltier elements, as the next section shows.

5.3. Self-Sufficient Peltier Heating Textiles

Peltier modules are often integrated into smart textiles for cooling, which is easier by thermoelectric cooling than by a vest in which a coolant liquid circulates [156–158]. A jacket that can heat or cool the wearer depending on the temperature was proposed by Poikayil et al.; however, no experiments were performed with the proposed design [42]. Generating a neutral microclimate under clothing by Peltier cells was investigated by Vlad et al., who found a drop in the relative humidity upon introducing Peltier cells due to an increased temperature of the textile layers, as well as constant skin temperature during exercise and rest [159]. The general possibility of using Peltier elements for heating was mentioned in several papers [157,160–163], but no studies of this possibility were found. No reports about tests on heating a volunteer or a thermal manikin by Peltier elements were found in the literature.

6. Applications of Energy-Self-Sufficient Heating Textiles—Chances and Limits

Some of the potential applications of energy-self-sufficient heating textiles were already mentioned in the previous sections. No papers mention the potential use of active heating textiles for homeless people. Using heated textiles to survive cold environments is at least scarcely mentioned [164–167].

Some studies investigated the possibility of using heated textiles for therapeutic applications, such as relieving joint and muscle pain [168], supporting wound healing by killing bacteria [169] or thermotherapy [170]. For sports and outdoor activities, mostly cooling textiles are investigated, but cooling/heating textiles are also investigated, often based on PCMs [171–173]. Another approach is the so-called personal thermal management, which can be applied in indoor situations to heat only a person's body, while the entire indoor space can be cooler to reduce energy consumption [174–176].

More applications, however, are related to working in extreme cold, such as the aforementioned space suits [22,135,155]. Li et al. generally suggested their heated textiles in the form of a garment, a seat and an insole for outdoor workers in winter [177], while many researchers concentrated on heated gloves for protection from extreme cold [178–180]. Depending on the specific environment and work, additional requirements have to be taken into account, such as fire resistance, flame-retardant properties, defined hydrophobic/hydrophilic properties, and windproof, fast-drying, isolating and other properties [156,181–183].

Most studies, however, exclude the long-term heating applications in which self-sufficient heating would really be necessary. To support people working and living under harsh environmental conditions, especially outdoor workers or homeless people during winter, this should be changed in future research studies.

7. Conclusions and Outlook

To create energy-self-sufficient heating textiles, it is necessary to integrate energy harvesting, energy storage and active heating in clothing. Different possibilities have

been investigated for energy harvesting, such as triboelectric nanogenerators (TENGs), photovoltaics, and thermoelectric or piezoelectric devices, and for energy storage, such as supercapacitors or batteries. Electric energy can be used to prepare Joule heating or Peltier heating textiles, while phase-change materials (PCMs) work independently from electric energy.

While all necessary components to prepare energy-self-sufficient active heating textiles are thus known and are being investigated by various research groups, there is still a lack of real-life tests on probands under harsh conditions or on thermal manikins under mostly realistic conditions. While most research groups aim at improving specific material parameters, only very few studies yet exist that measure the necessary energy to heat the inner part of a garment under defined environmental conditions towards a defined temperature for a given time. This makes it nearly impossible to estimate how long, e.g., the energy stored and saved in a garment during daytime could heat the clothing in the night, or how much energy must be stored in a working dress to enable active heating towards a defined temperature during a long outdoor working day under extremely cold conditions. Research on PCMs, on the other hand, clearly shows that they have recently only been suitable for short-term temperature variations, not for longer energy storage.

In the future, it is thus necessary to significantly increase the studies of active heating on a human volunteer or at least a thermal body manikin to gain more knowledge about the necessary energy for heating to a defined temperature under different environmental conditions.

To make lab experiments more comparable, heated textiles should be investigated under clearly defined, ideally standardized conditions, such as defined room temperature and relative humidity, and ideally freely held in the air instead of placed on an unknown underground to enable comparability across different studies. Since most of these experiments are performed with an infrared camera, it is necessary for all studies to mention the calibration of the emissivity, which strongly influences the measured temperatures [184]. In this way, comparability between different labs can significantly be increased, enabling more reliable measurements of material properties.

Author Contributions: Conceptualization, T.B., G.E. and E.S.-H.; methodology, T.B., I.K., E.S.-H. and A.E.; formal analysis, A.E.; investigation, M.M., I.K. and A.E.; writing—original draft preparation, T.B., M.M. and A.E.; writing—review and editing, all authors; visualization, G.E.; supervision, E.S.-H. All authors have read and agreed to the published version of the manuscript.

Funding: This research received no external funding.

Data Availability Statement: No new data were created for this review paper.

Conflicts of Interest: The authors declare no conflicts of interest.

References

1. Smith, M.H. Dress, Cloth, and the Farmer's Wife: Textiles from Ø 172 Tatsipataa, Greenland, with Comparative Data from Iceland. *J. North Atl.* **2014**, *2014*, 64–81. [[CrossRef](#)]
2. Yu, Y.F.; Zheng, G.C.; Dai, K.; Zhai, W.; Zhou, K.K.; Jia, Y.Y.; Zheng, G.J.; Zhang, Z.C.; Liu, C.T.; Shen, C.Y. Hollow-porous fibers for intrinsically thermally insulating textiles and wearable electronics with ultrahigh working sensitivity. *Mater. Horiz.* **2021**, *8*, 1037–1046. [[CrossRef](#)]
3. Jambrich, M.; Hodul, P. Textile applications of polypropylene fibers. In *Polypropylene*; Karger-Kocsis, J., Ed.; Springer: Dordrecht, The Netherlands, 1999; pp. 806–812.
4. Xie, A.-Q.; Zhu, L.L.; Liang, Y.Z.; Mao, J.; Liu, Y.J.; Chen, S. Fiber-spinning Asymmetric Assembly for Janus-structured Bifunctional Nanofiber Films towards All-Weather Smart Textile. *Angew. Chem.* **2022**, *134*, e202208592. [[CrossRef](#)]
5. Hsu, P.C.; Liu, C.; Song, A.Y.; Zhang, Z.; Peng, Y.; Xie, J.; Liu, K.; Wu, C.L.; Catrysse, P.B.; Cai, L.; et al. A dual-mode textile for human body radiative heating and cooling. *Sci. Adv.* **2017**, *3*, e1700895. [[CrossRef](#)]
6. Cai, L.; Song, A.Y.; Wu, P.; Hsu, P.C.; Peng, Y.; Chen, J.; Liu, C.; Catrysse, P.B.; Liu, Y.; Yang, A.; et al. Warming up human body by nanoporous metallized polyethylene textile. *Nat. Commun.* **2017**, *8*, 496. [[CrossRef](#)]
7. Peng, L.; Su, B.; Yu, A.; Jiang, X. Review of clothing for thermal management with advanced materials. *Cellulose* **2019**, *26*, 6415–6448. [[CrossRef](#)]
8. Peng, Y.; Cui, Y. Advanced textiles for personal thermal management and energy. *Joule* **2020**, *4*, 724–742. [[CrossRef](#)]

9. Zhang, Y.; Li, Y.; Li, K.Q.; Kwon, Y.S.; Tennakoon, T.; Wang, C.T.; Chan, K.C.; Fu, S.-C.; Huang, B.L.; Chao, C.Y.H. A large-area versatile textile for radiative warming and biomechanical energy harvesting. *Nano Energy* **2022**, *95*, 106996. [[CrossRef](#)]
10. Li, X.S.; Yang, Y.C.; Quan, Z.Z.; Wang, L.M.; Ji, D.X.; Li, F.X.; Qin, X.H.; Yu, J.Y.; Ramakrishna, S. Tailoring body surface infrared radiation behavior through colored nanofibers for efficient passive radiative heating textiles. *Chem. Eng. J.* **2022**, *430*, 133093. [[CrossRef](#)]
11. Ying, B.A.; Kwok, Y.L.; Li, Y.; Yeung, C.Y.; Zhu, Q.Y.; Li, F.Z. Computational Investigation of Thermoregulatory Effects of Multi-Layer PCM Textile Assembly. In *Computational Textile. Studies in Computational Intelligence*; Zeng, X., Li, Y., Ruan, D., Koehl, L., Eds.; Springer: Berlin/Heidelberg, Germany, 2007; Volume 55.
12. Gao, C. Phase-change materials (PCMs) for warming or cooling in protective clothing. In *Protective Clothing*; Woodhead Publishing Series in Textiles; Woodhead Publishing Ltd.: Cambridge, UK, 2014; pp. 227–249.
13. Ahrari, M.; Khajavi, R.; Dolatabadi, M.K.; Toliyat, T.; Rashidi, A. A Review on Application of Phase Change Materials in Textiles Finishing. *Int. J. Chem. Mol. Nucl. Mater. Metall. Eng.* **2017**, *11*, 400–405.
14. Choi, H.N.; Jee, S.H.; Ko, J.W.; Kim, D.J.; Kim, S.H. Properties of Surface Heating Textile for Functional Warm Clothing Based on a Composite Heating Element with a Positive Temperature Coefficient. *Nanomaterials* **2021**, *11*, 904. [[CrossRef](#)]
15. Thilagavathi, G.; Muthukumar, N.; Kannaian, T. Development and Characterization of Electric Heating Fabric Based on Silver Coated Nylon Yarn. *J. Text. Eng. Fash. Technol.* **2017**, *1*, 00036.
16. Wang, F.Q.; Liu, Y.M.; Yu, J.Y.; Li, Z.L.; Ding, B. Recent progress on general wearable electrical heating textiles enabled by functional fibers. *Nano Energy* **2024**, *124*, 109497. [[CrossRef](#)]
17. Faruk, M.O.; Ahmed, A.; Jalil, M.A.; Islam, M.T.; Shamim, A.M.; Adak, B.; Hossain, M.M.; Mukhopadhyay, S. Functional textiles and composite based wearable thermal devices for Joule heating: Progress and perspectives. *Appl. Mater. Today* **2021**, *23*, 101025. [[CrossRef](#)]
18. Hossain, M.T.; Shahid, M.A.; Ali, M.Y.; Saha, S.; Salman Ibna Jamal, M.; Habib, A. Fabrications, Classifications, and Environmental Impact of PCM-Incorporated Textiles: Current State and Future Outlook. *ACS Omega* **2023**, *8*, 45164–45176. [[CrossRef](#)]
19. Yang, K.; Venkataraman, M.; Zhang, X.L.; Wiener, J.; Zhu, G.C.; Yao, J.M.; Militky, J. Review: Incorporation of organic PCMs into textiles. *J. Mater. Sci.* **2022**, *57*, 798–847. [[CrossRef](#)]
20. Shin, Y.S.; Yoo, D.-I.; Son, K.H. Development of thermoregulating textile materials with microencapsulated phase change materials (PCM). IV. Performance properties and hand of fabrics treated with PCM microcapsules. *J. Appl. Polym. Sci.* **2005**, *97*, 910–915. [[CrossRef](#)]
21. Khadiran, T.; Hussein, M.Z.; Zainal, Z.; Rusli, R. Advanced energy storage materials for building applications and their thermal performance characterization: A review. *Renew. Sustain. Energy Rev.* **2016**, *57*, 916–928. [[CrossRef](#)]
22. Mondal, S. Phase change materials for smart textiles—An overview. *Appl. Therm. Eng.* **2008**, *28*, 1536–1550. [[CrossRef](#)]
23. Farid, M.M.; Khudhair, A.M.; Razack, S.A.K.; Al-Hallaj, S. A review on phase change energy storage: Materials and applications. *Energy Convers. Manag.* **2004**, *45*, 1597–1615. [[CrossRef](#)]
24. Bajaj, P. Thermally sensitive materials. In *Smart Fibres, Fabrics and Clothing*; Tao, X.M., Ed.; Woodhead Publishing Ltd.: Cambridge, UK, 2001; pp. 58–82.
25. Farid, M.M.; Kim, Y.; Kanzawa, A. Thermal performance of heat storage module using PCM's with different melting temperatures-experimental. *J. Sol. Energy Eng.* **1990**, *112*, 125–131. [[CrossRef](#)]
26. Feldman, D.; Shapiro, M.M. Fatty acids and their mixtures as phase-change materials for thermal energy storage. *Sol. Energy Mater.* **1989**, *18*, 201–216. [[CrossRef](#)]
27. Biswas, D.R. Thermal energy storage using sodium sulphate decahydrate and water. *Sol. Energy* **1977**, *19*, 99–100. [[CrossRef](#)]
28. Velraj, R.; Seeniraj, R.V.; Hafner, B.; Faber, C.; Schwarzer, K. Heat transfer enhancement in a latent heat storage system. *Sol. Energy* **1999**, *65*, 171–180. [[CrossRef](#)]
29. Hasnain, S.M. Review on sustainable thermal energy storage technologies, Part 1: Heat storage materials and techniques. *Energy Convers. Manag.* **1998**, *39*, 1127–1138. [[CrossRef](#)]
30. Py, X.; Olives, S.; Mauran, S. Paraffin/porous graphite matrix composite as a high and constant power thermal storage material. *Int. J. Heat Mass Transf.* **2001**, *44*, 2727–2737. [[CrossRef](#)]
31. Tan, F.L.; Hosseinzadeh, S.F.; Khodadadi, J.M.; Fan, L.W. Experimental and computational study of constrained melting of phase change materials (PCM) inside a spherical capsule. *Int. J. Heat Mass Transf.* **2009**, *52*, 3464–3472. [[CrossRef](#)]
32. Joulin, A.; Younsi, Z.; Zalewski, L.; Lassue, S.; Rousse, D.R.; Cavrot, J.-P. Experimental and numerical investigation of a phase change material: Thermal-energy storage and release. *Appl. Energy* **2011**, *88*, 2454–2456. [[CrossRef](#)]
33. Chen, C.; Guo, H.F.; Liu, Y.N.; Yue, H.L.; Wang, C.D. A new kind of phase change material (PCM) for energy-storing wallboard. *Energy and Buildings* **2008**, *40*, 882–890. [[CrossRef](#)]
34. Mazo, J.; El Badry, A.T.; Carreras, J.; Delgado, M.; Boer, D.; Zalba, B. Uncertainty propagation and sensitivity analysis of thermo-physical properties of phase change materials (PCM) in the energy demand calculations of a test cell with passive latent thermal storage. *Appl. Therm. Eng.* **2015**, *90*, 596–608. [[CrossRef](#)]
35. Tabor, J.; Chatterjee, K.; Ghosh, T.K. Smart textile-based personal thermal comfort systems: Current status and potential solutions. *Adv. Mater. Technol.* **2020**, *5*, 1901155. [[CrossRef](#)]
36. He, R.; Schierning, G.; Nielsch, K. Thermoelectric Devices: A Review of Devices, Architectures, and Contact Optimization. *Adv. Mater. Technol.* **2018**, *3*, 1700256. [[CrossRef](#)]

37. Chatterjee, K.; Ghosh, T.K. Thermoelectric Materials for Textile Applications. *Molecules* **2021**, *26*, 3154. [[CrossRef](#)] [[PubMed](#)]
38. Zhou, X.; Yan, Y.; Lu, X.; Zhu, H.; Han, X.; Chen, G.; Ren, Z. Routes for High-Performance Thermoelectric Materials. *Mater. Today* **2018**, *21*, 974–988. [[CrossRef](#)]
39. Zhao, L.-D.; Tan, G.; Hao, S.; He, J.; Pei, Y.; Chi, H.; Wang, H.; Gong, S.; Xu, H.; Dravid, V.P.; et al. Ultrahigh Power Factor and Thermoelectric Performance in Hole-Doped Single-Crystal SnSe. *Science* **2016**, *351*, 141–144. [[CrossRef](#)] [[PubMed](#)]
40. Vargiamidis, V.; Neophytou, N. Hierarchical Nanostructuring Approaches for Thermoelectric Materials with High Power Factors. *Phys. Rev. B* **2019**, *99*, 045405. [[CrossRef](#)]
41. Schmidl, G.; Gawlik, A.; Jia, G.; Andrä, G.; Richter, K.; Plentz, J. 3D spacer fabrics for thermoelectric textile cooling and energy generation based on aluminum doped zinc oxide. *Smart Mater. Struct.* **2020**, *29*, 125003. [[CrossRef](#)]
42. Poikayil, J.R.; Francis, J.; Saju, D.; Suresh, A.; Varghese, J. Peltier integrated heating & cooling jacket. In Proceedings of the 2017 International Conference of Electronics, Communication and Aerospace Technology (ICECA), Coimbatore, India, 20–22 April 2017; pp. 260–263.
43. Shi, Q.W.; Sun, J.Q.; Hou, C.Y.; Li, Y.G.; Zhan, Q.H.; Wang, H.Z. Advanced Functional Fiber and Smart Textile. *Adv. Fiber Mater.* **2019**, *1*, 3–31. [[CrossRef](#)]
44. Chen, G.R.; Li, Y.Z.; Bick, M.; Chen, J. Smart Textiles for Electricity Generation. *Chem. Rev.* **2020**, *120*, 3668–3720. [[CrossRef](#)]
45. Dong, K.; Hu, Y.F.; Yang, J.; Kim, S.-W.; Hu, W.G.; Wang, Z.L. Smart textile triboelectric nanogenerators: Current status and perspectives. *MRS Bull.* **2021**, *46*, 512–521. [[CrossRef](#)]
46. Qi, Y.; McAlpine, M.C. Nanotechnology-enabled flexible and biocompatible energy harvesting. *Energy Environ. Sci.* **2010**, *3*, 1275–1285. [[CrossRef](#)]
47. Ha, M.; Park, J.; Lee, Y.; Ko, H. Triboelectric generators and sensors for self-powered wearable electronics. *ACS Nano* **2015**, *9*, 3421–3427. [[CrossRef](#)] [[PubMed](#)]
48. Proto, A.; Penhaker, M.; Conforto, S.; Schmid, M. Nanogenerators for human body energy harvesting. *Trends Biotechnol.* **2017**, *35*, 610–624. [[CrossRef](#)]
49. Paosangthong, W.; Torah, R.; Beeby, S. Recent progress on textile-based triboelectric nanogenerators. *Nano Energy* **2019**, *55*, 401–423. [[CrossRef](#)]
50. Zhong, J.W.; Zhang, Y.; Zhong, Q.; Hu, Q.Y.; Hu, B.; Wang, Z.L.; Zhou, J. Fiber-Based Generator for Wearable Electronics and Mobile Medication. *ACS Nano* **2014**, *8*, 6273–6280. [[CrossRef](#)] [[PubMed](#)]
51. Jung, S.; Lee, J.; Hyeon, T.; Lee, M.; Kim, D.H. Fabric-based integrated energy devices for wearable activity monitors. *Adv. Mater.* **2014**, *26*, 6329–6334. [[CrossRef](#)]
52. Wang, S.; Liu, S.; Zhou, J.Y.; Li, F.X.; Li, J.; Cao, X.F.; Li, Z.Y.; Zhang, J.S.; Li, B.S.; Wang, Y.; et al. Advanced triboelectric nanogenerator with multi-mode energy harvesting and anti-impact properties for smart glove and wearable e-textile. *Nano Energy* **2020**, *78*, 105291. [[CrossRef](#)]
53. Lai, Y.-C.; Deng, J.; Zhang, S.L.; Niu, S.; Guo, H.; Wang, Z.L. Single-thread-based wearable and highly stretchable triboelectric nanogenerators and their applications in cloth-based self-powered human-interactive and biomedical sensing. *Adv. Funct. Mater.* **2017**, *27*, 1604462. [[CrossRef](#)]
54. He, T.Y.Y.; Shi, Q.F.; Wang, H.; Wen, F.; Chen, T.; Ouyang, J.Y.; Lee, C.K. Beyond energy harvesting—Multi-functional triboelectric nanosensors on a textile. *Nano Energy* **2019**, *57*, 338–352. [[CrossRef](#)]
55. Pu, X.; Song, W.; Liu, M.; Sun, C.; Du, C.; Jiang, C.; Huang, X.; Zou, D.; Hu, W.; Wang, Z.L. Wearable power-textiles by integrating fabric triboelectric nanogenerators and fiber-shaped dye-sensitized solar cells. *Adv. Energy Mater.* **2016**, *6*, 1601048. [[CrossRef](#)]
56. Tian, Z.; He, J.; Chen, X.; Zhang, Z.; Wen, T.; Zhai, C.; Han, J.; Mu, J.; Hou, X.; Chou, X.; et al. Performance-boosted triboelectric textile for harvesting human motion energy. *Nano Energy* **2017**, *39*, 562–570. [[CrossRef](#)]
57. Lee, S.; Ko, W.; Oh, Y.; Lee, J.; Baek, G.; Lee, Y.; Sohn, J.; Cha, S.; Kim, J.; Park, J.; et al. Triboelectric energy harvester based on wearable textile platforms employing various surface morphologies. *Nano Energy* **2015**, *12*, 410–418. [[CrossRef](#)]
58. Bayramol, D.V.; Soin, N.; Shah, T.; Siores, E.; Matsouka, D.; Vassiliadis, S. Energy Harvesting Smart Textiles. In *Smart Textiles. Human–Computer Interaction Series*; Schneegass, S., Amft, O., Eds.; Springer: Cham, Switzerland, 2017.
59. Kohn, S.; Wehlage, D.; Juhász Junger, I.; Ehrmann, A. Electrospinning a Dye-Sensitized Solar Cell. *Catalysts* **2019**, *9*, 975. [[CrossRef](#)]
60. Ehrmann, A.; Blachowicz, T. Recent coating materials for textile-based solar cells. *AIMS Mater.* **2019**, *6*, 234–251. [[CrossRef](#)]
61. Torah, R.; Lawrie-Ashton, J.; Li, Y.; Arumugam, S.; Sodano, H.A.; Beeby, S. Energy-harvesting materials for smart fabrics and textiles. *MRS Bull.* **2018**, *43*, 214–219. [[CrossRef](#)]
62. Plentz, J.; Andra, G.; Pliewischkies, T.; Brückner, U.; Eisenhauer, B.; Falk, F. Amorphous silicon thin-film solar cells on glass fiber textiles. *Mater. Sci. Eng. B* **2016**, *204*, 34–37. [[CrossRef](#)]
63. Jun, M.J.; Cha, S.I.; Seo, S.H.; Kim, H.S.; Lee, D.Y. Float printing deposition to control the morphology of TiO₂ photoanodes on woven textile metal substrates for TCO-free flexible dye-sensitized solar cells. *RSC Adv.* **2016**, *6*, 67331–67339.
64. Yun, M.J.; Cha, S.I.; Kim, H.S.; Seo, S.H.; Lee, D.Y. Monolithic-structured single-layered textile-based dye-sensitized solar cells. *Sci. Rep.* **2016**, *6*, 34249. [[CrossRef](#)] [[PubMed](#)]
65. Mamun, A.; Trabelsi, M.; Klöcker, M.; Sabantina, L.; Großhede, C.; Blachowicz, T.; Grötsch, G.; Cornelißen, C.; Streitenberger, A.; Ehrmann, A. Electrospun nanofiber mats with embedded non-sintered TiO₂ for dye-sensitized solar cells (DSSCs). *Fibers* **2019**, *7*, 60. [[CrossRef](#)]

66. Sánchez-García, M.A.; Bokhimi, X.; Velázquez Martínez, S.; Jiménez-González, A.E. Dye-Sensitized Solar Cells Prepared with Mexican Pre-Hispanic Dyes. *J. Nanotechnol.* **2018**, *2018*, 1236878. [CrossRef]
67. Juhász Junger, I.; Udomrungkajornchai, S.; Grimmelsmann, N.; Blachowicz, T.; Ehrmann, A. Effect of Caffeine Copigmentation of Anthocyanin Dyes on DSSC Efficiency. *Materials* **2019**, *12*, 2692. [CrossRef] [PubMed]
68. Desertec Foundation. An initiative of The Club of Rome. Clean Power from Deserts. The DESERTEC Concept for Energy, Water and Climate Security. WhiteBook, 4th ed. Available online: <https://actionguide.info/m/pubs/158/> (accessed on 30 March 2024).
69. Chai, Z.S.; Zhang, N.N.; Sun, P.; Huang, Y.; Zhao, C.X.; Fan, H.J.; Fan, X.; Mai, W.J. Tailorable and Wearable Textile Devices for Solar Energy Harvesting and Simultaneous Storage. *ACS Nano* **2016**, *10*, 9201–9207. [CrossRef]
70. Jeong, E.G.; Jeon, Y.M.; Cho, S.H.; Choi, K.C. Textile-based washable polymer solar cells for optoelectronic modules: Toward self-powered smart clothing. *Energy Environ. Sci.* **2019**, *12*, 1878–1889. [CrossRef]
71. Satharasinghe, A.; Hughes-Riley, T.; Dias, T. An investigation of a wash-durable solar energy harvesting textile. *Prog. Photovolt.* **2020**, *28*, 578–592. [CrossRef]
72. Ilén, E.; Elsehrawy, F.; Palovuori, E.; Halme, J. Washable textile embedded solar cells for self-powered wearables. *Res. J. Text. Appar.* **2024**, *28*, 133–151. [CrossRef]
73. Biancardo, M.; West, K.; Krebs, F.C. Optimizations of large area quasi-solid-state dye-sensitized solar cells. *Sol. Energy Mater. Sol. Cells* **2006**, *90*, 2575–2588. [CrossRef]
74. Pope, J.; Lekakou, C. Thermoelectric polymer composite yarns and an energy harvesting wearable textile. *Smart Mater. Struct.* **2019**, *28*, 095006. [CrossRef]
75. Siddique, A.R.M.; Mahmud, S.; van Heyst, B. A review of the state of the science on wearable thermoelectric power generators (TEGs) and their existing challenges. *Renew. Sustain. Energy Rev.* **2017**, *73*, 730–744. [CrossRef]
76. Settaluri, K.T.; Lo, H.; Ram, R.J. Thin thermoelectric generator system for body energy harvesting. *J. Electron. Mater.* **2012**, *41*, 984–988. [CrossRef]
77. Stark, I. Converting body heat into reliable energy for powering physiological wireless sensors. In Proceedings of the 2nd Conference on Wireless Health WH '11, San Diego/La Jolla, CA, USA, 10–13 October 2011; ACM Press: New York, NY, USA, 2011.
78. Lund, A.; Tian, Y.; Darabi, S.; Müller, C. A polymer-based textile thermoelectric generator for wearable energy harvesting. *J. Power Sources* **2020**, *480*, 228836. [CrossRef]
79. Elmoughni, H.M.; Menon, A.K.; Wolfe, R.M.W.; Yee, S.K. A Textile-Integrated Polymer Thermoelectric Generator for Body Heat Harvesting. *Adv. Mater. Technol.* **2019**, *4*, 1800708. [CrossRef]
80. Finefrock, S.W.; Zhu, X.Q.; Sun, Y.M.; Wu, Y. Flexible prototype thermoelectric devices based on Ag₂Te and PEDOT:PSS coated nylon fibre. *Nanoscale* **2015**, *7*, 5598–5602. [CrossRef] [PubMed]
81. Ding, Y.F.; Qiu, Y.; Cai, K.F.; Yao, Q.; Chen, S.; Chen, L.D.; He, J.Q. High performance n-type Ag₂Se film on nylon membrane for flexible thermoelectric power generator. *Nat. Comm.* **2019**, *10*, 841. [CrossRef] [PubMed]
82. Liu, J.; Jia, Y.H.; Jiang, Q.L.; Jiang, F.X.; Li, C.C.; Wang, X.D.; Liu, P.; Liu, P.P.; Hu, F.; Du, Y.K.; et al. Highly Conductive Hydrogel Polymer Fibers toward Promising Wearable Thermoelectric Energy Harvesting. *ACS Appl. Mater. Interfaces* **2018**, *10*, 44033–44040. [CrossRef] [PubMed]
83. Lee, J.A.; Aliev, A.E.; Bykova, J.S.; Jung de Andrade, M.; Kim, D.Y.; Sim, H.J.; Lepró, X.; Zakhidov, A.A.; Lee, J.-B.; Spinks, G.M.; et al. Woven-Yarn Thermoelectric Textiles. *Adv. Mater.* **2016**, *28*, 5038–5044. [CrossRef] [PubMed]
84. Wang, L.M.; Zhang, K. Textile-Based Thermoelectric Generators and Their Applications. *Energy Environ. Mater.* **2020**, *3*, 67–79. [CrossRef]
85. Hossain, I.Z.; Khan, A.; Hossain, G. A Piezoelectric Smart Textile for Energy Harvesting and Wearable Self-Powered Sensors. *Energies* **2022**, *15*, 5541. [CrossRef]
86. Wu, J.; Mahajan, A.; Riekehr, L.; Zhang, H.; Yang, B.; Meng, N. Nano Energy for high power energy storage. *Nano Energy* **2018**, *50*, 723–732. [CrossRef]
87. Feng, Z.B.; Zhao, Z.Q.; Liu, Y.N.; Liu, Y.K.; Cao, X.Y.; Yu, D.-G.; Wang, K. Piezoelectric Effect Polyvinylidene Fluoride (PVDF): From Energy Harvester to Smart Skin and Electronic Textiles. *Adv. Mater. Technol.* **2023**, *8*, 2300021. [CrossRef]
88. Liu, Z.H.; Pan, C.T.; Lin, L.W.; Huang, J.C.; Ou, Z.Y. Direct-write PVDF nonwoven fiber fabric energy harvesters via the hollow cylindrical near-field electrospinning process. *Smart Mater. Struct.* **2013**, *23*, 025003. [CrossRef]
89. Dolez, P.I. Energy Harvesting Materials and Structures for Smart Textile Applications: Recent Progress and Path Forward. *Sensors* **2021**, *21*, 6297. [CrossRef] [PubMed]
90. Matsouka, D.; Vassiliadis, S.; Prekas, K.; Bayramol, D.V.; Soin, N.; Siores, E. On the Measurement of the Electrical Power Produced by Melt Spun Piezoelectric Textile Fibres. *J. Electron. Mater.* **2016**, *45*, 5112–5126. [CrossRef]
91. Koç, M.; Paralı, L.; Şan, O. Fabrication and vibrational energy harvesting characterization of flexible piezoelectric nanogenerator (PEN) based on PVDF/PZT. *Polym. Test.* **2020**, *90*, 106695. [CrossRef]
92. Jeerapan, I.; Sempionatto, J.R.; Wang, J. On-body bioelectronics: Wearable biofuel cells for bioenergy harvesting and self-powered biosensing. *Adv. Funct. Mater.* **2020**, *30*, 1906243. [CrossRef]
93. Gao, Y.; Cho, J.H.; Ryu, J.H.; Choi, S.H. A scalable yarn-based biobattery for biochemical energy harvesting in smart textiles. *Nano Energy* **2020**, *74*, 104897. [CrossRef]
94. Lv, J.; Jeerapan, I.; Tehrani, F.; Yin, L.; Silva-Lopez, C.A.; Jang, J.-H.; Joshua, D.; Shah, R.; Liang, Y.Y.; Xie, L.Y.; et al. Sweat-based wearable energy harvesting-storage hybrid textile devices. *Energy Environ. Sci.* **2018**, *11*, 3431–3442. [CrossRef]

95. Zhai, S.L.; Karahan, H.E.; Wie, L.; Qian, Q.H.; Harris, A.T.; Minett, A.I.; Ramakrishna, S.; Ng, A.K.; Chen, Y. Textile energy storage: Structural design concepts, material selection and future perspectives. *Energy Storage Mater.* **2016**, *3*, 123–139. [[CrossRef](#)]
96. Duan, Y.X.; You, G.C.; Sun, K.; Zhu, Z.; Liao, X.Q.; Lv, L.F.; Tang, H.; Xu, B.; He, L. Advances in wearable textile-based micro energy storage devices: Structuring, application and perspective. *Nanoscale Adv.* **2021**, *3*, 6271–6293. [[CrossRef](#)] [[PubMed](#)]
97. Huang, Q.Y.; Wang, D.R.; Zheng, Z.J. Textile-Based Electrochemical Energy Storage Devices. *Adv. Energy Mater.* **2016**, *6*, 1600783. [[CrossRef](#)]
98. Cheng, H.Y.; Li, Q.; Zhu, L.L.; Chen, S. Graphene Fiber-Based Wearable Supercapacitors: Recent Advances in Design, Construction, and Application. *Small Methods* **2021**, *5*, 2100502. [[CrossRef](#)]
99. Bai, B.; Qiu, L.L.; Yuan, Y.F.; Song, L.X.; Xiong, J.; Du, P.F. Nitrogen doped siloxene and composite with graphene for high performance fiber-based supercapacitors. *J. Energy Storage* **2023**, *63*, 106984. [[CrossRef](#)]
100. Xu, Y.F.; Lu, W.B.; Xu, G.B.; Chou, T.-W. Structural supercapacitor composites: A review. *Compos. Sci. Technol.* **2021**, *204*, 108636. [[CrossRef](#)]
101. Ma, W.J.; Li, W.F.; Li, M.; Mao, Q.H.; Pan, Z.H.; Hu, J.; Li, X.; Zhu, M.F.; Zhang, Y.G. Unzipped Carbon Nanotube/Graphene Hybrid Fiber with Less “Dead Volume” for Ultrahigh Volumetric Energy Density Supercapacitors. *Adv. Funct. Mater.* **2021**, *31*, 2100195. [[CrossRef](#)]
102. Wang, P.Z.; Du, X.X.; Wang, X.J.; Zhang, K.W.; Sun, J.H.; Chen, Z.; Xia, Y.Z. Integrated fiber electrodes based on marine polysaccharide for ultrahigh-energy-density flexible supercapacitors. *J. Power Sourc.* **2021**, *506*, 230130. [[CrossRef](#)]
103. He, C.; Cheng, J.L.; Liu, Y.H.; Zhang, X.C.; Wang, B. Thin-walled hollow fibers for flexible high energy density fiber-shaped supercapacitors. *Energy Mater.* **2021**, *1*, 100010. [[CrossRef](#)]
104. Nie, G.D.; Luan, Y.X.; Kou, Z.K.; Jiang, J.M.; Zhang, Z.Y.; Yang, N.; Wang, J.; Long, Y.-Z. Fiber-in-tube and particle-in-tube hierarchical nanostructures enable high energy density of MnO₂-based asymmetric supercapacitors. *J. Colloid Interface Sci.* **2021**, *582*, 543–551. [[CrossRef](#)] [[PubMed](#)]
105. Dong, X.M.; Liang, J.C.; Li, H.; Wu, Z.T.; Zhang, L.; Deng, Y.G.; Yu, H.Y.; Tao, Y.; Yang, Q.-H. Matching electrode lengths enables the practical use of asymmetric fiber supercapacitors with a high energy density. *Nano Energy* **2021**, *80*, 105523. [[CrossRef](#)]
106. Ren, C.L.; Yan, Y.S.; Sun, B.Z.; Gu, B.H.; Chou, T.-W. Wet-spinning assembly and in situ electrodeposition of carbon nanotube-based composite fibers for high energy density wire-shaped asymmetric supercapacitor. *J. Colloid Interface Sci.* **2020**, *569*, 298–306. [[CrossRef](#)]
107. Manjakkal, L.; Franco, F.F.; Pullanchiyodan, A.; González-Jiménez, M.; Dahiya, R. Natural Jute Fibre-Based Supercapacitors and Sensors for Eco-Friendly Energy Autonomous Systems. *Adv. Sust. Syst.* **2021**, *5*, 2000286. [[CrossRef](#)]
108. Zheng, X.H.; Hu, Q.L.; Zhou, X.S.; Nie, W.G.; Li, C.L.; Yuan, N.Y. Graphene-based fibers for the energy devices application: A comprehensive review. *Mater. Des.* **2021**, *201*, 109476. [[CrossRef](#)]
109. Tang, M.; Wu, Y.; Yang, J.; Xue, Y. Hierarchical core-shell fibers of graphene fiber/radially-aligned molybdenum disulfide nanosheet arrays for highly efficient energy storage. *J. Alloys Compd.* **2020**, *828*, 135622. [[CrossRef](#)]
110. Sundriyal, P.; Bhattacharya, S. Textile-based supercapacitors for flexible and wearable electronic applications. *Sci. Rep.* **2020**, *10*, 13259. [[CrossRef](#)] [[PubMed](#)]
111. Sha, Z.; Huang, F.; Zhou, Y.; Zhang, J.; Wu, S.Y.; Chen, J.Y.; Brown, S.A.; Peng, S.H.; Han, Z.J.; Wang, C.-H. Synergies of vertical graphene and manganese dioxide in enhancing the energy density of carbon fibre-based structural supercapacitors. *Compos. Sci. Technol.* **2021**, *201*, 108568. [[CrossRef](#)]
112. Wen, X.; Jiang, K.; Zhang, H.; Huang, H.; Yang, L.Y.; Zhou, Z.Y.; Weng, Q.H. Flexible and Wearable Zinc-Ion Hybrid Supercapacitor Based on Double-Crosslinked Hydrogel for Self-Powered Sensor Application. *Materials* **2022**, *15*, 1767. [[CrossRef](#)] [[PubMed](#)]
113. Khadem, A.H. Recent Advances in Functional Fabric-Based Wearable Supercapacitors. *Adv. Mater. Interfaces* **2024**, *11*, 2300724. [[CrossRef](#)]
114. Su, C.L.; Shao, G.W.; Yu, Q.H.; Huang, Y.L.; Jiang, J.H.; Shao, H.Q.; Chen, N.L. A flexible, lightweight and stretchable all-solid-state supercapacitor based on warp-knitted stainless-steel mesh for wearable electronics. *Text. Res. J.* **2022**, *92*, 1807–1819. [[CrossRef](#)]
115. Yu, J.H.; Wu, J.F.; Wang, H.Z.; Zhou, A.; Huang, C.Q.; Bai, H.; Li, L. Metallic Fabrics as the Current Collector for High-Performance Graphene-Based Flexible Solid-State Supercapacitor. *ACS Appl. Mater. Interfaces* **2016**, *8*, 4724–4729. [[CrossRef](#)]
116. Zhang, Q.; Liu, D.; Pei, H.Y.; Pan, W.; Liu, Y.L.; Xu, S.G.; Cao, S.K. Swelling-reconstructed chitosan-viscose nonwoven fabric for high-performance quasi-solid-state supercapacitors. *J. Colloid Interface Sci.* **2022**, *617*, 489–499. [[CrossRef](#)] [[PubMed](#)]
117. Wen, J.F.; Xu, B.G.; Zhou, J.Y. Towards 3D knitted-fabric derived supercapacitors with full structural and functional integrity of fiber and electroactive materials. *J. Power Sources* **2020**, *473*, 228559. [[CrossRef](#)]
118. Zheng, X.H.; Wang, Y.; Nie, W.Q.; Wang, Z.Q.; Hu, Q.L.; Li, C.L.; Wang, P.; Wang, W. Elastic polyaniline nanoarrays/MXene textiles for all-solid-state supercapacitors and anisotropic strain sensors. *Compos. Part A Appl. Sci. Manuf.* **2022**, *158*, 106985. [[CrossRef](#)]
119. Zuo, W.S.; Zang, L.M.; Liu, Q.F.; Qiu, J.H.; Lan, M.Y.; Yang, C. A quasi-solid-state supercapacitor based on waste surgical masks with high flexibility and designable shape. *Colloids Surf. A Physicochem. Eng. Asp.* **2022**, *634*, 128020. [[CrossRef](#)]
120. Lin, X.; Li, X.; Zhang, Z.; Li, X.; Zhang, W.; Xu, J.; Song, K. Screen-printed water-based conductive ink on stretchable fabric for wearable micro-supercapacitor. *Mater. Today Chem.* **2023**, *30*, 101529. [[CrossRef](#)]
121. Mo, F.N.; Liang, G.J.; Huang, Z.D.; Li, H.F.; Wang, D.H.; Zhi, C.Y. An Overview of Fiber-Shaped Batteries with a Focus on Multifunctionality, Scalability, and Technical Difficulties. *Adv. Mater.* **2020**, *32*, 1902151. [[CrossRef](#)]

122. Zhao, C.L.; Lu, Y.X.; Chen, L.Q.; Hu, Y.-S. Flexible Na batteries. *InfoMat* **2020**, *2*, 126–138. [[CrossRef](#)]
123. Zhou, Z.Y.; Zeng, T.T.; Zhang, H.R.; Chen, D. Mesoporous VCN Nanobelts for High-Performance Flexible Zn-Ion Batteries. *Energies* **2022**, *15*, 4932. [[CrossRef](#)]
124. Xiao, X.; Xiao, X.; Zhou, Y.; Zhao, X.; Chen, G.; Liu, Z.; Wang, Z.; Lu, C.; Hu, M.; Nashalian, A.; et al. An ultrathin rechargeable solid-state zinc ion fiber battery for electronic textiles. *Sci. Adv.* **2021**, *7*, eabl3742. [[CrossRef](#)] [[PubMed](#)]
125. Li, M.; Li, Z.Q.; Ye, X.R.; Zhang, X.J.; Qu, L.J.; Tian, M.W. Tendril-Inspired 900% Ultrastretching Fiber-Based Zn-Ion Batteries for Wearable Energy Textiles. *ACS Appl. Mater. Interfaces* **2021**, *13*, 17110–17117. [[CrossRef](#)]
126. Gao, Y.; Xie, C.; Zheng, Z.J. Textile Composite Electrodes for Flexible Batteries and Supercapacitors: Opportunities and Challenges. *Adv. Energy Mater.* **2021**, *11*, 2002838. [[CrossRef](#)]
127. Ali, A.E.; Jeoti, V.; Stojanovic, G.M. Fabric based printed-distributed battery for wearable e-textiles: A review. *Sci. Technol. Adv. Mater.* **2021**, *22*, 772–793. [[CrossRef](#)]
128. Chen, X.Y.; Gao, H.; Tian, X.J.; Wu, D.S.; Lv, P.F.; Yoon, S.S.; Yang, J.X.; Wei, Q.F. Tunable fabric zinc-based batteries utilizing core-shell like fiber electrodes with enhanced deformation durability. *Nano Energy* **2024**, *125*, 109501. [[CrossRef](#)]
129. Gu, Z.-Y.; Guo, J.-Z.; Sun, Z.-H.; Zhao, X.-X.; Li, W.-H.; Yang, X.; Liang, H.-J.; Zhao, C.-D.; Wu, X.-L. Carbon-coating-increased working voltage and energy density towards an advanced $\text{Na}_3\text{V}_2(\text{PO}_4)_2\text{F}_3$ @C cathode in sodium-ion batteries. *Sci. Bull.* **2020**, *65*, 702–710. [[CrossRef](#)]
130. Chong, S.K.; Yang, J.; Sun, L.; Guo, S.W.; Liu, Y.N.; Liu, H.K. Potassium Nickel Iron Hexacyanoferrate as Ultra-Long-Life Cathode Material for Potassium-Ion Batteries with High Energy Density. *ACS Nano* **2020**, *14*, 9807–9818. [[CrossRef](#)]
131. Wang, D.H.; Han, C.P.; Mo, F.N.; Yang, Q.; Zhao, Y.W.; Li, Q.; Liang, G.J.; Dong, B.B.; Zhi, C.Y. Energy density issues of flexible energy storage devices. *Energy Storage Mater.* **2020**, *28*, 264–292. [[CrossRef](#)]
132. Mäkinen, M. Introduction to phase change materials. In *Intelligent Textiles and Clothing*; Mattila, I.H.R., Ed.; Woodhead Publishing: Cambridge, UK, 2006; pp. 21–33.
133. Tyurin, I.N.; Getmantseva, V.V.; Andreeva, E.G. Analysis of Innovative Technologies of Thermoregulating Textile Materials. *Fibre Chem.* **2018**, *50*, 1–9. [[CrossRef](#)]
134. Kizildag, N. Smart textiles with PCMs for thermoregulation. In *Multifunctional Phase Change Materials*; Woodhead Publishing: Cambridge, UK, 2023; pp. 445–505.
135. Zhang, Y.H.; Li, T.S.; Zhang, S.H.; Jiang, L.; Xia, J.; Xie, J.Y.; Chen, K.F.; Bao, L.X.; Lei, J.X.; Wang, J.L. Room-temperature, energy storage textile with multicore-sheath structure obtained via in-situ coaxial electrospinning. *Chem. Eng. J.* **2022**, *436*, 135226. [[CrossRef](#)]
136. Yan, Y.R.; Li, W.P.; Zhu, R.T.; Lin, C.; Hufenus, R. Flexible Phase Change Material Fiber: A Simple Route to Thermal Energy Control Textiles. *Materials* **2021**, *14*, 401. [[CrossRef](#)]
137. Pause, B. Nonwoven Protective Garments with Thermo-Regulating Properties. *J. Ind. Text.* **2003**, *33*, 93–99. [[CrossRef](#)]
138. Li, F.Z. Numerical simulation for effects of microcapsuled phase change material (mpcm) distribution on heat and moisture transfer in porous textiles. *Mod. Phys. Lett. B* **2009**, *23*, 501–504.
139. Ying, B.-A.; Kwok, Y.-L.; Li, Y.; Zhu, Q.-Y.; Yeung, C.-Y. Assessing the performance of textiles incorporating phase change materials. *Polym. Test.* **2004**, *23*, 541–549. [[CrossRef](#)]
140. Hamdan, H.; Ghaddar, N.; Ouahrani, D.; Ghali, K.; Itani, M. PCM cooling vest for improving thermal comfort in hot environment. *Int. J. Therm. Sci.* **2016**, *102*, 154–167. [[CrossRef](#)]
141. Ghali, K.; Ghaddar, N.; Harathani, J.; Jones, B. Experimental and Numerical Investigation of the Effect of Phase Change Materials on Clothing During Periodic Ventilation. *Text. Res. J.* **2004**, *74*, 205–214. [[CrossRef](#)]
142. Behzadi, S.; Farid, M.M. Long term thermal stability of organic PCMs. *Appl. Energy* **2014**, *122*, 11–16. [[CrossRef](#)]
143. Johansen, J.B.; Englmaier, G.; Dannemand, M.; Kong, W.Q.; Fan, J.H.; Dragsted, J.; Perers, B.; Furbo, S. Laboratory testing of solar combi system with compact long term PCM heat storage. *Energy Procedia* **2016**, *91*, 330–337. [[CrossRef](#)]
144. Chen, W.; Zhou, G.B. Numerical investigation on thermal performance of a solar greenhouse with synergetic energy release of short- and long-term PCM storage. *Sol. Energy* **2024**, *269*, 112313. [[CrossRef](#)]
145. Deka, P.P.; Ansu, A.K.; Sharma, R.K.; Tyagi, V.V.; Sari, A. Development and characterization of form-stable porous TiO_2 /tetradecanoic acid based composite PCM with long-term stability as solar thermal energy storage material. *Int. J. Energy Res.* **2020**, *44*, 10044–10057. [[CrossRef](#)]
146. Huang, Z.W.; Luo, Z.G.; Gao, X.N.; Fang, X.M.; Fang, Y.T.; Zhang, Z.G. Investigations on the thermal stability, long-term reliability of LiNO_3/KCl —Expanded graphite composite as industrial waste heat storage material and its corrosion properties with metals. *Appl. Energy* **2017**, *188*, 521–528. [[CrossRef](#)]
147. De Castro, P.F.; Minko, S.; Vinokurov, V.; Cherednichenko, K.; Shchukin, D.G. Long-Term Autonomic Thermoregulating Fabrics Based on Microencapsulated Phase Change Materials. *ACS Appl. Energy Mater.* **2021**, *4*, 12789–12797. [[CrossRef](#)]
148. Ding, Y.L.; Dong, H.H.; Cao, J.; Zhang, Z.; Chen, R.H.; Wang, Y.; Yan, J.; Liao, Y.P. A polyester/spandex blend fabrics-based e-textile for strain sensor, joule heater and energy storage applications. *Compos. Part A Appl. Sci. Manuf.* **2023**, *175*, 107779. [[CrossRef](#)]
149. Guo, Z.P.; Wang, Y.L.; Huang, J.J.; Zhang, S.Y.; Zhang, R.Q.; Ye, D.Z.; Cai, G.M.; Yang, H.J.; Gu, S.J.; Xu, W.L. Multi-functional and water-resistant conductive silver nanoparticle-decorated cotton textiles with excellent joule heating performances and human motion monitoring. *Cellulose* **2021**, *28*, 7483–7495. [[CrossRef](#)]

150. Ma, J.H.; Zhao, Q.L.; Zhou, Y.X.; He, P.X.; Pu, H.H.; Song, B.G.; Pan, S.X.; Wang, Y.W.; Wang, C. Hydrophobic wrapped carbon nanotubes coated cotton fabric for electrical heating and electromagnetic interference shielding. *Polym. Test.* **2021**, *100*, 107240. [[CrossRef](#)]
151. Zhang, D.B.; Yin, R.; Zheng, Y.J.; Li, Q.M.; Liu, H.; Liu, C.T.; Shen, C.Y. Multifunctional MXene/CNTs based flexible electronic textile with excellent strain sensing, electromagnetic interference shielding and Joule heating performances. *Chem. Eng. J.* **2022**, *438*, 135587. [[CrossRef](#)]
152. Dong, J.C.; Tang, X.W.; Peng, Y.D.; Fan, C.H.; Li, L.; Zhang, C.; Lai, F.L.; He, G.J.; Ma, P.M.; Wang, Z.C.; et al. Highly permeable and ultrastretchable E-textiles with EGaln-superlyophilicity for on-skin health monitoring, joule heating, and electromagnetic shielding. *Nano Energy* **2023**, *108*, 108194. [[CrossRef](#)]
153. Shuvo, I.I.; Decaens, J.; Dolez, P.I. Characterization method of the Joule heating efficiency of electric textiles and influence of boundary conditions. *Flex. Print. Electron.* **2023**, *8*, 025010. [[CrossRef](#)]
154. Song, W.F.; Zhang, C.J.; Lai, D.D.; Wang, F.M.; Kuklane, K. Use of a novel smart heating sleeping bag to improve wearers' local thermal comfort in the feet. *Sci. Rep.* **2016**, *6*, 19326. [[CrossRef](#)] [[PubMed](#)]
155. Tian, Y.S.; Li, D.; Liu, H.Q. The Relationship between Active Heating Power and Temperature of the Fingers in EVA Glove. In *HCI International 2014—Posters' Extended Abstracts. HCI 2014. Communications in Computer and Information Science*; Stephanidis, C., Ed.; Springer: Cham, Switzerland, 2014; Volume 434.
156. Revaiah, R.G.; Kotresh, T.M.; Kandasubramanian, B. Technical textiles for military applications. *J. Text. Inst.* **2020**, *111*, 273–308. [[CrossRef](#)]
157. Sajjad, U.; Hamid, K.; Sultan, M.; Abbas, N.; Ali, H.M.; Imran, M.; Muneeshwaran, M.; Chang, J.Y.; Wang, C.C. Personal thermal management—A review on strategies, progress, and prospects. *Int. Commun. Heat Mass Transf.* **2022**, *130*, 105739. [[CrossRef](#)]
158. Wei, W.; Wu, B.; Guo, Y.; Hu, Y.H.; Liao, Y.H.; Wu, C.M.; Zhang, Q.H.; Li, Y.G.; Chen, J.H.; Hou, C.Y.; et al. A multimodal cooling garment for personal thermal comfort management. *Appl. Energy* **2023**, *352*, 121973. [[CrossRef](#)]
159. Vlad, L.; Mitu, S.; Buhai, C. Optimizing the Thermal Physiological Comfort by Introducing Peltier Cells in Simulated Conditions. *Appl. Mech. Mater.* **2013**, *371*, 792–796. [[CrossRef](#)]
160. Chen, X.Y.; Yang, X.N.; Han, X.; Ruan, Z.P.; Xu, J.C.; Huang, F.L.; Zhang, K. Advanced Thermoelectric Textiles for Power Generation: Principles, Design, and Manufacturing. *Glob. Chall.* **2024**, *8*, 2300023. [[CrossRef](#)] [[PubMed](#)]
161. Yang, X.N.; Zhang, K. Direct Wet-Spun Single-Walled Carbon Nanotubes-Based p - n Segmented Filaments toward Wearable Thermoelectric Textiles. *ACS Appl. Mater. Interfaces* **2022**, *14*, 44704–44712. [[CrossRef](#)]
162. Scott, R.A. The technology of electrically heated clothing. *Ergonomics* **1988**, *31*, 1065–1081. [[CrossRef](#)]
163. Mikolajczyk, Z.; Szalek, A. Thermal Analysis of Heating–Cooling Mat of Textile Incubator for Infants. *Autex Res. J.* **2021**, *21*, 305–322. [[CrossRef](#)]
164. Zhang, X.A.; Yu, S.; Xu, B.; Li, M.; Peng, Z.; Wang, Y.; Deng, S.; Wu, X.; Wu, Z.; Ouyang, M.; et al. Dynamic gating of infrared radiation in a textile. *Science* **2019**, *363*, 619–623. [[CrossRef](#)] [[PubMed](#)]
165. McCann, J. Identification of design requirements for smart clothes and wearable technology. In *Smart Clothes and Wearable Technology*, 2nd ed.; The Textile Institute Book Series; Elsevier: Amsterdam, The Netherlands, 2023; pp. 327–369.
166. Cui, Y.; Gong, H.X.; Wang, Y.J.; Li, D.W.; Bai, H. A Thermally Insulating Textile Inspired by Polar Bear Hair. *Adv. Mater.* **2018**, *30*, 1706807. [[CrossRef](#)] [[PubMed](#)]
167. Holmér, I. Textiles for protection against cold. In *Textiles for Protection*; Scott, R.A., Ed.; Woodhead Publishing Ltd.: Cambridge, UK, 2005; pp. 378–397.
168. Maurya, S.K.; Somkuwar, V.U.; Das, A.; Kumar, N.; Kumar, B. Influence of Knitting Engineering and Environment Conditions on the Performance of Heating Textiles for Therapeutic Applications. *ACS Appl. Eng. Mater.* **2023**, *1*, 1644–1654. [[CrossRef](#)]
169. Zhao, X.; Wang, L.-Y.; Tang, C.-Y.; Zha, X.-J.; Liu, Y.; Su, B.-H.; Ke, K.; Bao, R.-Y.; Yang, M.-B.; Yang, W. Smart $\text{Ti}_3\text{C}_2\text{T}_x$ MXene Fabric with Fast Humidity Response and Joule Heating for Healthcare and Medical Therapy Applications. *ACS Nano* **2020**, *14*, 8793–8805. [[CrossRef](#)] [[PubMed](#)]
170. Zhu, S.H.; Lou, C.-W.; Zhang, S.H.; Wang, N.; Li, J.W.; Feng, Y.J.; He, R.D.; Xu, C.G.; Lin, J.-H. Clean surface additive manufacturing of aramid paper-based electrically heated devices for medical therapy application. *Surf. Interfaces* **2022**, *29*, 101689. [[CrossRef](#)]
171. Scataglini, S.; Moorhead, A.P.; Feletti, F. A Systematic Review of Smart Clothing in Sports: Possible Applications to Extreme Sports. *Muscles Ligaments Tendons J.* **2020**, *10*, 333–342. [[CrossRef](#)]
172. McCann, J. Sports applications. In *Polyesters and Polyamides*; Woodhead Publishing Series in Textiles; Woodhead Publishing Ltd.: Cambridge, UK, 2008; pp. 505–524.
173. Mbise, E.; Dias, T.; Hurley, W.; Morris, R. The study of applying heat to enhance moisture transfer in knitted spacer structures. *J. Ind. Text.* **2017**, *47*, 1584–1608. [[CrossRef](#)]
174. Prakash, B.J.; Jahar, S.; Pralay, M. Review on passive daytime radiative cooling: Fundamentals, recent researchers, challenges and opportunities. *Renew. Sustain. Energy Rev.* **2020**, *133*, 110263.
175. Zhu, F.L.; Feng, Q.Q. Recent advances in textile materials for personal radiative thermal management in indoor and outdoor environments. *Int. J. Therm. Sci.* **2021**, *165*, 106899. [[CrossRef](#)]
176. Tang, L.T.; Lyu, B.; Gao, D.G.; Jia, Z.T.; Ma, Z.J. A wearable textile with superb thermal functionalities and durability towards personal thermal management. *Chem. Eng. J.* **2023**, *465*, 142829. [[CrossRef](#)]

177. Li, S.S.; Deng, Y.; Cao, B. Study on the Performance of Personal Heating in Extremely Cold Environments Using a Thermal Manikin. *Buildings* **2023**, *13*, 362. [[CrossRef](#)]
178. Ducharme, M.B.; Brajkovic, D.; Frim, J. The effect of direct and indirect hand heating on finger blood flow and dexterity during cold exposure. *J. Therm. Biol.* **1999**, *24*, 391–396. [[CrossRef](#)]
179. Brajkovic, D.; Ducharme, M.B. Finger dexterity, skin temperature, and blood flow during auxiliary heating in the cold. *J. Appl. Physiol.* **2003**, *95*, 758–770. [[CrossRef](#)]
180. Ma, L.; Li, J. A review on active heating for high performance cold-proof clothing. *Int. J. Cloth. Sci. Technol.* **2023**, *35*, 952–970. [[CrossRef](#)]
181. Li, F.; Ren, P. Influences of Anti-G Suit Material Hygroscopicity on Thermal Stress Index of the Pilot. In Proceedings of the First International Conference on Information Sciences, Machinery, Materials and Energy, Chongqing, China, 11–13 April 2015; Atlantis Press: Beijing, China, 2015; pp. 603–608.
182. Yang, C.Q.; Yang, H. The Flame Retardant Nomex/Cotton and Nylon/Cotton Blend Fabrics for Protective Clothing. In *Advances in Modern Woven Fabrics Technology*, Vassiliadis, S., Ed.; IntechOpen: London, UK, 2011; pp. 197–210.
183. Shekar, R.I.; Kotresh, T.M.; Subbulakshmi, M.S.; Vijayalakshmi, S.N.; Prasad, A.S.K. Thermal Resistance Properties of Paratrooper Clothing. *J. Ind. Text.* **2009**, *39*, 123–148. [[CrossRef](#)]
184. Höser, D.; Wallimann, R.; Von Rohr, P.R. Uncertainty Analysis for Emissivity Measurement at Elevated Temperatures with an Infrared Camera. *Int. J. Thermophys.* **2016**, *37*, 14. [[CrossRef](#)]

Disclaimer/Publisher’s Note: The statements, opinions and data contained in all publications are solely those of the individual author(s) and contributor(s) and not of MDPI and/or the editor(s). MDPI and/or the editor(s) disclaim responsibility for any injury to people or property resulting from any ideas, methods, instructions or products referred to in the content.